

Accepted Manuscript

Title: Towards a siRNA-containing nanoparticle targeted to breast cancer cells and the tumor microenvironment

Authors: Lígia C. Gomes-da-Silva, Adriana O. Santos, Luís M. Bimbo, Vera Moura, José S. Ramalho, Maria C. Pedroso de Lima, Sérgio Simões, João N. Moreira



PII: S0378-5173(12)00502-9
DOI: doi:10.1016/j.ijpharm.2012.05.018
Reference: IJP 12602

To appear in: *International Journal of Pharmaceutics*

Received date: 26-2-2012
Revised date: 6-5-2012
Accepted date: 11-5-2012

Please cite this article as: Gomes-da-Silva, L.C., Santos, A.O., Bimbo, L.M., Moura, V., Ramalho, J.S., Lima, M.C.P., Simões, S., Moreira, J.N., Towards a siRNA-containing nanoparticle targeted to breast cancer cells and the tumor microenvironment, *International Journal of Pharmaceutics* (2012), doi:10.1016/j.ijpharm.2012.05.018

This is a PDF file of an unedited manuscript that has been accepted for publication. As a service to our customers we are providing this early version of the manuscript. The manuscript will undergo copyediting, typesetting, and review of the resulting proof before it is published in its final form. Please note that during the production process errors may be discovered which could affect the content, and all legal disclaimers that apply to the journal pertain.

1 **Towards a siRNA-containing nanoparticle targeted to breast cancer cells and the**
2 **tumor microenvironment**

3
4 Lígia C. Gomes-da-Silva ^{a,b}, Adriana O. Santos ^{a,b}, Luís M. Bimbo ^{a,b}, Vera Moura ^{a,b},
5 José S. Ramalho ^c, Maria C. Pedroso de Lima ^{b,d}, Sérgio Simões ^{a,b}, João N. Moreira ^{a,b,*}

6
7 ^a Faculty of Pharmacy, University of Coimbra, Portugal

8 ^b Center for Neurosciences and Cell Biology, University of Coimbra, Portugal

9 ^c Laboratory of Cellular and Molecular Biology, Faculty of Medical Sciences, New
10 University of Lisbon, Portugal

11 ^d Department of Life Sciences, Faculty of Sciences and Technology, University of
12 Coimbra, Portugal

13 * Corresponding author. João Nuno Moreira, Center for Neurosciences and Cell
14 Biology, University of Coimbra, Largo Marquês de Pombal, 3004-517 Coimbra,
15 Portugal. E-mail: jmoreira@ff.uc.pt. Mobile phone: +351 916885272

16
17 **Abstract**

18 The present work aimed at designing a lipid-based nanocarrier for siRNA delivery
19 towards two cell sub-populations within breast tumors, the cancer and the endothelial
20 cells from angiogenic tumor blood vessels. To achieve such goal, the F3 peptide, which
21 is specifically internalized by nucleolin overexpressed on both those sub-populations,
22 was used as a targeting moiety.

23 The developed F3-targeted stable nucleic acid lipid particles presented adequate features
24 for systemic administration. In addition, the attachment of the F3 peptide onto the
25 liposomal surface enabled an internalization by both cancer and endothelial cells from
26 angiogenic blood vessels that was significantly higher than the one observed with non-
27 cancer cells. Sequence-specific downregulation of enhanced green fluorescent protein
28 (eGFP) in *eGFP*-overexpressing human cancer cell lines, both at the protein and mRNA
29 levels, was further observed upon delivery of anti-*eGFP* siRNA by F3-targeted
30 liposomes, in contrast with the non-targeted counterpart. This effect was highly
31 dependent on the content of poly(ethylene glycol) (PEG), as evidenced by the co-
32 localization studies between the siRNA and lysosomes.

33 Overall, the present work represents an important contribution towards a nanoparticle
34 with multi-targeting capabilities in breast cancer, both at the cellular and molecular
35 level.

36

37 **Keywords:** dual-targeted delivery, ligand-mediated targeting, Stable Nucleic Acid
38 Lipid Particles (SNALP), siRNA, breast cancer.

39

40 **1. Introduction**

41 Cancer is still a severe public health problem being one of the most deadly diseases in
42 the western world (Jemal et al., 2011). The limited effectiveness of conventional
43 treatment strategies has generated considerable interest on the development of novel
44 anticancer agents, with improved molecular target specificity. In this context, small-
45 interfering RNA (siRNA), 21-23 nucleotides long double-stranded RNA that inhibit the
46 expression of a target gene through specific cleavage of perfectly complementary
47 mRNA (Elbashir et al., 2001a; Elbashir et al., 2001b; Fire et al., 1998), may constitute a
48 novel class of pharmaceutical drugs, as they can potently and specifically inhibit the
49 expression of any intracellular protein involved in tumor initiation and/or progression.
50 However, the translation of these molecules from the bench to the clinic has been
51 hindered by their limited cellular uptake, low biological stability and unfavorable
52 pharmacokinetics (Castanotto and Rossi, 2009; Moreira et al., 2008).

53 In order to overcome the mentioned limitations, different types of poly(ethylene glycol)
54 (PEG)-grafted liposomes have been developed such as, stabilized antisense lipid
55 particles (SALP) (Maurer et al., 2001; Semple et al., 2001), or the related stabilized
56 nucleic acid lipid particles (SNALP) encapsulating siRNA (Akinc et al., 2010; Geisbert
57 et al., 2006; Judge et al., 2009; Morrissey et al., 2005; Zimmermann et al., 2006). The
58 PEG-derivatized lipid in the liposomal formulation forms a hydrophilic shell around the
59 liposomes that, upon intravenous administration, decreases the rate and the extent of
60 electrostatic and hydrophobic interactions between the surface of liposomes and blood
61 components that mediate liposomal blood clearance (Allen and Hansen, 1991; Allen et
62 al., 1991; Papahadjopoulos et al., 1991). In addition, those systems are also
63 characterized by high nucleic acid encapsulation, nucleic acid protection from serum
64 nucleases, a small average size, and a net charge close to neutrality, thus making them
65 adequate for intravenous administration. Although pegylated systems can exhibit
66 passive accumulation into a tumor due to their large fenestrated endothelium (enhanced

67 permeability and retention, EPR, effect (Fang et al., 2011; Iyer et al., 2006)), large
68 improvements can be achieved through the covalent attachment of internalizing
69 targeting ligands, which will interact specifically with receptors overexpressed on the
70 surface of target cells (Moreira et al., 2008; Torchilin, 2010).

71 However, the design of novel targeted anticancer strategies must take into account that
72 the aggressiveness of a tumor does not rely only on the cancer cell, but rather on the
73 cross-talk between cancer cells and other cells from the tumor microenvironment such
74 as, the endothelial cells (Hanahan and Weinberg, 2011). Thus, targeting angiogenesis,
75 in addition to cancer cells, can significantly improve clinical efficacy, as tumor growth
76 and metastases formation are angiogenesis-dependent (Abdollahi and Folkman, 2010).
77 Furthermore, vascular targeting carries some additional advantages since endothelial
78 cells are more accessible (than cancer cells) to the therapeutic agent injected in the
79 vascular compartment, and are less prone to acquire drug resistance. In addition,
80 treatment selectivity can be achieved, as, besides tumors, the formation of new blood
81 vessels is restricted to a few physiological processes such as wound healing, ovulation
82 and pregnancy (Abdollahi and Folkman, 2010).

83 The F3 peptide, which is specifically internalized by nucleolin, a receptor overexpressed
84 on the surface of cancer and endothelial cells of tumor blood vessels, offers the
85 possibility to develop dual-targeting strategies for nucleic acid delivery (Christian et al.,
86 2003; Porkka et al., 2002).

87 Therefore, the main aim of this work was to design F3-targeted SNALP for the
88 encapsulation, protection and effective intracellular delivery of siRNA to two cell
89 populations within a tumor: the cancer cells and the endothelial cells from angiogenic
90 blood vessels.

91

92 **2. Materials and methods**

93 **2.1 Materials**

94 Lipids, 1,2-dioleoyl-3-dimethylammonium-propane (DODAP), 1,2-distearoyl-*sn*-
95 glycerol-3-phosphocholine (DSPC), N-Palmitoyl-Sphingosine-1-
96 [Succinyl(MethoxyPolyethylene Glycol)₂₀₀₀] (CerC₁₆-PEG₂₀₀₀), 1,2-Distearoyl-*sn*-
97 Glycerol-3-Phosphatidylethanolamine-N-[Maleimide (Polyethylene Glycol)₂₀₀₀]
98 ammonium salt (DSPE-PEG-MAL) and L- α -Phosphoethanolamine-N-(lissamine
99 rhodamine B sulfonyl) (Rho-PE) were purchased from Avanti Polar Lipids (USA). The
100 lipid, cholesterol (CHOL), was obtained from Sigma (Germany).

101 The anti-*eGFP* siRNA (5'GAA CUU CAG GGU CAG CUU GCdTdT -3'), the control
102 siRNA (5' - GUC UCA AGU UUU CGG GAA GdTdT -3') and the FITC-labelled anti-
103 *eGFP* siRNA were purchased from Dharmacon (USA).

104 The 31 aminoacid F3 peptide (KDEPQRRSARLSAKPAPPKPEPKPKKAPAKK) and
105 the non-specific (NS) peptide were purchased from Genecust (Luxembourg) (Porkka et
106 al., 2002).

107

108 **2.2 Cell lines**

109 The human breast cancer cell lines, MDA-MB-435S and MDA-MB-231, and the human
110 fibroblasts, BJ, were from American Type Culture Collection (ATCC). The human
111 microvascular endothelial cell line, HMEC-1, was a generous gift from the Center for
112 Disease Control and Prevention (USA).

113 MDA-MB-435S and MDA-MB-231 were cultured in RPMI 1640 medium (Sigma,
114 Germany) and human fibroblasts cells, BJ, were cultured in DMEM medium (Sigma,
115 Germany). Both media were supplemented with 10% (v/v) heat-inactivated foetal
116 bovine serum (Invitrogen, USA), and 100 U/ml penicillin, 100 µg/ml streptomycin
117 (Invitrogen, USA). HMEC-1 cells were cultured in RPMI 1640 supplemented with 10
118 ng/ml of mouse epidermal growth factor (mEGF) (Sigma, Germany) and 1 µg/ml
119 hydrocortisone (Sigma, Germany). Cells were maintained in exponential growth phase,
120 at 37°C, in a 90% humidified atmosphere containing 5% CO₂.

121

122 **2.3 Preparation of sterically stabilized liposomes**

123 Preparation of stabilized nucleic acid lipid particles (SNALP) was adapted from Semple
124 et al. (Maurer et al., 2001; Semple et al., 2001). A lipid mixture of
125 DODAP:DSPC:CHOL:CerC₁₆-PEG₂₀₀₀ (30:23:45:2, 30:21:45:4 or 30:15:45:8, % molar
126 ratio relative to total lipid, 13 µmol) in absolute ethanol and 0.046 µmol of anti-*eGFP*
127 siRNA or of a non-specific siRNA in 20 mM citrate buffer, pH 4, were heated at 65°C.
128 For cellular association and internalization studies, nanoparticles were double-labelled
129 with anti-*eGFP* FITC-labelled siRNA and 1 mol % of Rho-PE.

130 The lipid mixture was added, slowly and under strong agitation, to the siRNA solution.
131 The resulting particles were then extruded 21 times through polycarbonate membranes
132 of 100 nm pore diameter, using a LiposoFast basic extruder (Avestin, Canada).
133 Removal of ethanol and non-encapsulated siRNA was carried out upon running

134 extruded nanoparticles through a Sepharose CL-4B column equilibrated with HEPES
135 buffered saline (HBS) (20 mM HEPES, 145 mM NaCl), pH 7.4.

136

137 **2.4 Preparation of targeted liposomes**

138 Targeted liposomes were prepared by the post-insertion method (Moreira et al., 2002;
139 Santos et al., 2010). Briefly, F3 and NS peptides were first thiolated upon reaction with
140 2-iminothiolane in HBS, pH 8, during 1 h at room temperature, in an inert N₂
141 atmosphere. They were then coupled to DSPE-PEG-MAL micelles, prepared in MES
142 buffered saline (MBS) (20 mM MES, 20 mM HEPES), pH 6.5. Insertion of DSPE-
143 PEG-MAL-F3 or DSPE-PEG-MAL-NS conjugates onto the preformed sterically
144 stabilized liposomes previously prepared, took place upon incubation of the
145 corresponding micelles with the latter at 50°C for 1 h. For the non-targeted lipid
146 particles, post-insertion was performed only with plain DSPE-PEG-MAL micelles.
147 Neutralization of non-reacted maleimide groups was performed upon incubation with 2-
148 mercaptoethanol at a maleimide/2-mercaptoethanol molar ratio of 1:5. Finally,
149 liposomes were run through a Sepharose CL-4B column equilibrated with HBS, pH 7.4.

150

151 **2.5 Characterization of the liposomes**

152 The final total lipid concentration was inferred from the cholesterol concentration,
153 determined with the Infinity[®] liquid stable reagent (Thermo Scientific, USA). The
154 quantification of the siRNA that was encapsulated into the liposomes was determined
155 with the Quanti-iT[™] Ribogreen reagent (Invitrogen, USA), in the presence of
156 octaethylene glycol monododecyl ether (C₁₂E₈) detergent (Sigma, Germany). The
157 encapsulation efficiency was calculated from the formula $[(\text{siRNA}/\text{total lipid})_{\text{final molar}} / (\text{siRNA}/\text{total lipid})_{\text{initial molar}}] \times 100$. In order to assess if the siRNA was fully
158 encapsulated and protected by the lipid nanoparticle, the ability of the probe Quanti-iT[™]
159 Ribogreen to intercalate with siRNA, in the absence of the detergent C₁₂E₈, was
160 evaluated.

162 The mean diameter of the resulting liposomes was determined by Photon Correlation
163 Spectroscopy, using a N5 submicron particle size analyser (Beckman Coulter). The zeta
164 potential was assessed using a Particle Size Analyzer 90 Plus (Brookhaven).

165 To determine the amount of DSPE-PEG-MAL-F3 conjugate that was transferred onto
166 the preformed liposomes, the F3 peptide was quantified using the CBQCA protein
167 quantification Kit (Invitrogen, USA).

168

169 2.6 Assessment of cellular association by flow cytometry

170 Half million of cancer, fibroblast or endothelial cells were seeded in 48-well plate.
171 Twenty four hours later, cells were incubated at 37 or 4°C, during 1 h, with rhodamine-
172 labelled F3-targeted, NS-targeted or non-targeted liposomes, at 0.2, 0.4 or 0.6 mM of
173 total lipid. Afterwards, cells were washed three times with phosphate buffer saline
174 (PBS), pH 7.4, detached with dissociation buffer and immediately analyzed by flow
175 cytometry using a FACS Calibur flow cytometer (BD, Biosciences). Rhodamine
176 fluorescence was evaluated in the FL2 channel and a total of 20.000 events were
177 collected. Data were analyzed with the Cell Quest Pro software.

178

179 2.7 Assessment of cellular internalization by confocal fluorescence microscopy

180 For the confocal studies, 2.5×10^5 of cancer, fibroblast or endothelial cells were seeded
181 on glass cover slips in 12-well plate and further incubated, at 37 or 4°C, during 1 h, with
182 1 μ M of FITC-labelled siRNA encapsulated in rhodamine-labelled liposomes (F3-
183 targeted or non-targeted). After washing three times with PBS, cells were fixed with 4%
184 paraformaldehyde, and the nucleus stained with DAPI, washed with PBS, and finally,
185 mounted in mowiol mounting medium. Confocal images were acquired in a Zeiss LSM-
186 510 point scanning confocal microscope (Zeiss, Germany), using a diode (405 nm), an
187 argon (488 nm) and a DPSS excitations lasers for DAPI, FITC and Rhodamine,
188 respectively, and a 63x oil immersion objective. Images were acquired and analyzed
189 using the LSM 510 Meta software. All instrumental parameters pertaining to
190 fluorescence detection and images analyses were held constant to allow sample
191 comparison.

192

193 2.8 Evaluation of eGFP levels by flow cytometry

194 Human cancer cell lines overexpressing eGFP, MDA-MB-435S-eGFP and MDA-MB-
195 231-eGFP, were used to evaluate the potential of the F3-targeted liposomes to
196 downregulate a target protein. EGFP was used as a model target as its downregulation
197 could be easily assessed upon measuring fluorescence by flow cytometry, thus
198 facilitating the assessment of the delivery properties of each one of the formulations to
199 be tested.

200 In order to evaluate the downregulation of eGFP, 30.000 cells were seeded in 48-well
201 plates. Twenty-four hours later, cells were transfected, at 37°C during 4 h, with different

202 concentrations of anti-*eGFP* siRNA encapsulated in F3-targeted or non-targeted
203 liposomes, or a non-specific siRNA encapsulated in the former. Afterwards, cell culture
204 medium was replaced with fresh medium and a second transfection was performed 44 h
205 after the beginning of the experiment, with the same formulations and concentrations
206 used in the first transfection. In another set of experiments, single transfections were
207 performed right at the beginning of the experiment, at 37°C during 4 h. In these
208 experiments, 48 or 96 h after the beginning of the experiment, cells were detached and
209 *eGFP* levels were evaluated by flow cytometry using a FACS Calibur flow cytometer
210 (BD, Biosciences).

211 *EGFP* fluorescence was evaluated in the FL1 channel and a total of 20,000 events were
212 collected. Data were then analyzed with the Cell Quest Pro software. The *eGFP*
213 fluorescence reduction was expressed in percentage of the ratio: $100 - [(eGFP \text{ signal of}$
214 $\text{treated cells}/eGFP \text{ signal of untreated cells}) \times 100]$.

215

216 **2.9 Intracellular trafficking of siRNA encapsulated in F3-targeted liposomes**

217 In order to investigate whether siRNA encapsulated in the developed F3-targeted
218 liposomes could efficiently escape from endosomes, co-localization studies between the
219 siRNA and lysosomes were performed in MDA-MB-435S cells.

220 Cancer cells were seeded on μ -slide 8-well ibitreat plates (Ibidi, Germany). After 24 h,
221 cells were incubated with F3-targeted liposomes encapsulating a FITC-labelled siRNA,
222 during 4 h at 37°C. Afterwards, lysosomes were stained upon cell incubation with 100
223 nM LysoTracker Red (Invitrogen, USA) for 2 h, followed by washing three times with
224 PBS. Live cells were then immediately visualized using an argon (488 nm), a DPSS
225 (561 nm) and a helium-neon (633 nm) excitations lasers for FITC, LysoTracker Red and
226 differential interference contrast (DIC), respectively, and a 63x oil immersion objective.
227 Images were acquired and analyzed as previously described.

228

229 **2.10 Evaluation of *eGFP* mRNA by quantitative real-time reverse-transcription** 230 **PCR (qRT-PCR)**

231 In order to confirm that the eGFP reduction observed by flow cytometry was due to an
232 RNA interference mechanism, the levels of *eGFP* mRNA were determined by qRT-
233 PCR, 24 h after the second transfection (72 h after the beginning of the experiment).
234 Cells were harvested and RNA extracted with RNeasy Mini Kit (Qiagen, Germany)
235 according to the manufacturer's instructions. The Quanti-iT™ Ribogreen reagent was
236 used to quantify the extracted RNA, where 0.5 µg of RNA was reversed transcribed into
237 cDNA in a 20 µl reaction mixture using the SuperSript™ III First Strand Synthesis
238 Supermix (Invitrogen, USA) following the manufacturer's instructions.
239 Quantitative real-time PCR (q-PCR) was performed using the Iq™SYBR Green
240 Supermix (Bio-Rad, USA). *Beta-2-microglobulin* (*β2M*) was used as the endogenous
241 control (housekeeping gene). The forward primer for *β2M* was 5'-
242 GAGTATGCCTGCCGTGTG-3' and the reverse primer was 5'-
243 AATCCAAATGCGGCATCT-3' (Microsynth, Switzerland). For *eGFP*, the
244 QuantiTect™ Primer Assay (Qiagen, Germany) was used.
245 The optimized qPCR conditions included the activation of HotStartTaq Plus DNA
246 polymerase followed by 40 cycles of two steps: a first step of denaturation (10 s at 95°C)
247 and a second step of combined annealing/extension (30 s at 60°C). After the qPCR, a
248 melting curve analysis of the PCR products was performed to confirm their specificity.
249 The threshold cycle (Ct) values were generated by the iQ5 Optical System Software.
250 The level of *eGFP* mRNA was calculated by the Livak method, $2^{-\Delta\Delta Ct} \times 100$, where
251 $\Delta\Delta Ct = (Ct\ eGFP - Ct\ \beta2M)\ \text{treated} - (Ct\ eGFP - Ct\ \beta2M)\ \text{untreated}$. The application
252 of this method relied on the similar PCR efficiencies between the target gene and the
253 housekeeping gene.

254

255 **2.11 Statistical analysis**

256 The results are presented as the mean ± standard deviation (SD) of at least three
257 independent experiments. One- or two-way ANOVA with Bonferroni's post-test was
258 used to determine statistically significant differences of the means. Statistical
259 differences are presented at probability levels of $p > 0.05$, $p < 0.05$, $p < 0.01$, and $p < 0.001$.

260

261 **3. Results**

262 **3.1 Preparation and physico-chemical characterization of F3-targeted and non-** 263 **targeted liposomes**

264 The pharmacokinetics and biodistribution of any encapsulated drug, regardless its
265 nature, are highly dependent on the physico-chemical properties of the liposomes,
266 including size, surface charge, level of protection against nucleases and the presence of
267 targeting moieties at the surface that are specifically recognized by internalizing
268 receptors overexpressed on the target cells (Li and Huang, 2008).

269 It is well recognized that PEG plays an important role preventing particle aggregation
270 during the preparation process (Maurer et al., 2001). Therefore the impact of the
271 incorporation of different amounts of CerC₁₆-PEG₂₀₀₀ (2, 4, and 8 mol% relative to total
272 lipid) on the final size of the liposomes was evaluated. For F3-targeted liposomes, an
273 increase in the amount of the PEG-derivatized lipid, from 2 to 4%, led to a decrease on
274 the mean size of the particles reaching values around 200 nm, while exhibiting a narrow
275 particle distribution as the polydispersity index was in the range of 0.14 - 0.15 (Table
276 1). We have also verified that the length of the encapsulated siRNA influenced the
277 liposomal mean size. A difference as small as 1 nt on the siRNA length, has resulted in
278 a reduction of around 50 nm in the mean size of targeted liposomes with 2 mol% of
279 CerC₁₆-PEG₂₀₀₀ (205.70 ± 18.55 nm).

280 The attachment of the F3 peptide to the surface of liposomes was performed by the
281 insertion (Ishida et al., 1999; Moreira et al., 2002) of DSPE-PEG-MAL-F3 conjugates
282 onto preformed liposomes, leading to an average amount of 4 nmol of F3 peptide per
283 μ mol of total lipid. Importantly, this procedure has not interfered with the loading of the
284 encapsulated nucleic acids since encapsulation efficiencies close to 100% have been
285 observed for both non-targeted and F3-targeted liposomes (Table 1). This high siRNA
286 encapsulation efficiency was certain due to the inclusion in the lipid bilayer of the
287 ionizable lipid DODAP, which is positively charged at low pH. However, after siRNA
288 encapsulation, adjustment of the external pH to neutral pH resulted in nanoparticles
289 close to neutrality, which reduces their ability to interact with serum proteins that
290 mediate an early clearance from the blood stream (Li and Huang, 2008). Non-targeted
291 liposomes were slightly negative (-4.83 ± 1.23 mV) while F3-targeted liposomes ($0.37 \pm$
292 3.48 mV) exhibit a net surface charge close to neutrality likely due to the presence of
293 the F3 peptide on the surface of the particle, which is rich in lysines and thus positively
294 charged.

295 Regarding the level of nucleic acid protection in both formulations tested, it was
296 observed that in the absence of the membrane-disrupting detergent C₁₂E₈, the probe
297 Quant-iTTM Ribogreen was not able to intercalate with the encapsulated siRNA,

298 translated in levels of protection close to 100%. These results indicated that the
299 nanoparticles were efficiently playing one of their primary roles, which consist in the
300 protection against nuclease-mediated degradation.

301

302 Insert Table 1

303

304 **3.2 Cellular association studies**

305 At 37°C, the level of cellular association of F3-targeted liposomes was significantly
306 higher than the one observed for the non-targeted liposomes or liposomes coupled to a
307 non-specific peptide. These results indicated that the presence of the F3 peptide at the
308 liposomal surface brought an important gain, as it mediated an important improvement
309 on the extent of cellular association by breast cancer cells, including the triple negative
310 MDA-MB-231 cells, and the endothelial cells from angiogenic blood vessels, HMEC-1
311 as well (Marchio et al., 2004).

312 Upon incubation with 0.4 mM of total lipid, a 12-fold or a 14-fold increase in the
313 rhodamine signal for both MDA-MB-231 and HMEC-1 cells or MDA-MB-435S cell
314 lines, respectively, was observed. Regardless the histological origin of the cells, the
315 cellular uptake was dose-dependent (Figure 1 A).

316 The interaction of the developed F3-targeted liposomes revealed to be peptide-specific
317 as it was pointed out by the low level of cellular association observed with the
318 liposomes coupled to a non-specific peptide. Moreover, in similar experiments
319 performed with a non-cancer (negative control) cell line, BJ fibroblasts, the previous
320 mentioned differences between F3-targeted and non-targeted liposomes were dissipated,
321 thus indicating that the interaction of the former with the target cells was also tumor
322 cell-specific. This observation is of high relevance as it strongly indicated that the
323 proposed strategy would avoid the internalization by normal tissues, thus reducing its
324 potential toxicity (Figure 1 A).

325 Incubation of F3-targeted liposomes at 4°C, a temperature non-permissive for
326 endocytosis, strongly inhibited cellular association when compared to incubations at 37
327 °C, a condition where both binding and endocytosis take place. These results suggested
328 that an energy-dependent process, most likely receptor-mediated endocytosis, was
329 involved in the uptake of F3-targeted liposomes (Figure 1 B).

330

331 Insert Fig. 1

332

333 In order to confirm the previous results, additional cellular association studies were
334 performed and cells analyzed by confocal microscopy. After 1 h of incubation, F3-
335 targeted liposomes were localized in the cytoplasm of cancer (MDA-MB-435S and
336 MDA-MB-231) and endothelial cells (HMEC-1), as can be observed by the intense red
337 and green fluorescence, from rhodamine (marker of the liposomal membrane) and FITC
338 (labelling the encapsulated nucleic acid), respectively. This pattern was not visible
339 neither in the non-cancer BJ fibroblasts nor when any of the tested cells were incubated
340 with non-targeted liposomes. In addition, when MDA-MB-435S cells were incubated
341 with F3-targeted liposomes, at 4°C, no significant levels of internalization were
342 observed (Figure 2). Overall, these findings corroborate the previous results observed
343 by flow cytometry thus, also reinforcing the cell-specific interaction of the developed
344 targeted liposomes.

345

346 Insert Fig. 2

347 **3.4 Evaluation of eGFP levels**

348 For proof-of-concept on the intracellular delivery capabilities of each one of the tested
349 formulations, MDA-MB-435 and MDA-MB-231 cells overexpressing the *enhanced*
350 *green fluorescence protein (eGFP)* were used, along with a siRNA against *eGFP*.

351 When cells were transfected twice with anti-*eGFP* siRNA delivered by F3-targeted
352 liposomes incorporating 2 mol% of CerC₁₆-PEG₂₀₀₀ (Figure 3 A, B), a significant
353 concentration-dependent downregulation of the target protein was observed in both
354 MDA-MB-435S (from 19.9 to 42.7%) and MDA-MB-231 (from 17.9 to 29.9%), upon
355 assessment at 96 h after the beginning of the experiment. These results emphasized the
356 importance of the intracellular delivery of the nucleic acid on its activity, as a total
357 absence of eGFP silencing was registered with the non-targeted counterpart. The
358 difference on the extent of eGFP silencing between these two cell lines, was likely
359 related with the higher extent of cellular association (and internalization) by the MDA-
360 MB-435S cells (Figures 1 and 2).

361 Interestingly, for the same 96 h duration of the experiment no significant differences in
362 the level of eGFP silencing were observed upon performing a single transfection
363 (Figure 3 A, B). Moreover, eGFP signal reduction in MDA-MB-435S-eGFP, 48 h after
364 one single transfection, was lower than the one observed at 96 h (22.3 *versus* 36.1%, at

365 2 μ M siRNA; $p < 0.001$) (Figure 3 A, C). Taken together, these results reflect the ability
366 of the siRNA to be recycled intracellularly over time, thus propagating gene silencing
367 (Hutvagner and Zamore, 2002) and, the low turnover of the target protein as well (Li et
368 al., 1998). The siRNA concentrations required with the proposed F3-targeted strategy
369 were higher than the ones used with regular agents for in *vitro* transfection, like
370 lipofectamine (data not shown), however, they were in accordance with other reports on
371 ligand-mediated targeted (PEGylated) liposomes for the delivery of nucleic acids (Di
372 Paolo et al., 2011; Mendonca et al., 2010).

373 In order to assess if liposomes with a higher PEG content and therefore more stable
374 from a physical point of view, still maintained the capacity to silence a target protein,
375 MDA-MB-435S-eGFP cells were transfected with anti-*eGFP* siRNA delivered by F3-
376 targeted liposomes incorporating 4 or 8 mol% of CerC₁₆-PEG₂₀₀₀. Transfection with 4
377 mol% of PEG F3-targeted liposomes still enabled downregulation of the target protein
378 (Figure 3 D) but to a lesser extent than the counterpart incorporating 2 mol% PEG
379 (Figure 3 A), whereas the presence of 8 mol% PEG completely prevented gene
380 silencing (data not shown). In MDA-MB-231-eGFP cells a total absence of eGFP
381 silencing was observed even with targeted liposomes incorporating 4 mol% PEG (data
382 not shown). These results were likely related with the lower extent of liposomal uptake
383 by the MDA-MB-231, relative to the MDA-MB-435.

384 In all the experiments performed, none of the tested formulations had a significant
385 impact on cell viability (data not shown).

386

387 Insert Fig 3

388

389 **3.5 The inhibitory effect of PEG on the cellular association and intracellular** 390 **trafficking**

391 To better understand the effect of PEG on the transfection efficiency, we have first
392 evaluated the extent of cellular association of F3-targeted liposomes incorporating 2 or
393 8 mol% of PEG. In fact, a slight decrease on the level of cellular association was
394 observed for the formulation incorporating the highest amount of PEG (Figure 4).
395 However, these results did not explain per se the absence of protein downregulation
396 associated with this formulation, as significant extent of association with the target cells
397 was still achieved.

398 Being aware of how critical an efficient endosomal escape is for nucleic acids
399 bioavailability and pharmacodynamics, the co-localization between FITC-labelled
400 siRNA (green), delivered by each of those nanoparticles, with lysotracker red-labelled
401 lysosomes (red) was assessed following an incubation period of 4 h. The strong yellow
402 staining following incubation with targeted liposomes prepared with 8 mol% of PEG,
403 suggested a higher extent of co-localization between siRNA and lysosomes (Figure 5
404 A). In contrast, following delivery by liposomes with 2 mol% of PEG, a decrease on the
405 intensity of the yellow staining suggested a decrease on the extent of co-localization
406 (Figure 5 B). Overall, these results suggested that the high content of PEG strongly
407 impair the siRNA endosomal escape, thus justifying the lack of activity of anti-*eGFP*
408 siRNA delivered by F3-targeted liposomes incorporating 8 mol% of PEG.

409

410 Insert Fig 4

411

412 Insert Fig 5

413

414 **3.6 Evaluation of *eGFP* mRNA by qRT-PCR**

415 Incubation of MDA-MB-435S-*eGFP* cells with F3-targeted liposomes containing the
416 anti-*eGFP* siRNA led to an effective impact at the mRNA level, achieving a
417 downregulation of 50% at 2 μ M siRNA. This effect was dependent on the siRNA
418 concentration (Figure 6), as was also observed at the protein level by flow cytometry
419 (Figure 3). With non-targeted liposomes containing the anti-*eGFP* siRNA or F3-
420 targeted liposomes containing a control siRNA, no significant downregulation of *eGFP*
421 mRNA was observed (Figure 6), evidencing both the molecular specificity of this
422 approach and the importance of the intracellular delivery as well. Overall, these results
423 pointed out the strong benefit of F3-targeted liposomes as a platform for the delivery of
424 siRNA.

425

426 Insert Fig 6

427

428 **4. Discussion**

429 As a therapeutic approach, gene silencing molecules, and particularly siRNA, provide
430 solutions to the major drawbacks of traditional pharmaceutical drugs. The principal
431 advantage over small molecules and protein therapeutics are that all targets, including
432 'non-druggable' targets, can be inhibited by siRNA, which can be rapidly and rationally
433 screened, designed and synthesized (Bumcrot et al., 2006).

434 Although siRNAs are one of the most promising class of RNAi mediators for
435 therapeutic purposes, the clinical advancement of this strategy has been difficult to
436 reach. This is particularly relevant when intravenous administration is envisaged as
437 naked siRNAs are easily degraded by blood nucleases, rapidly eliminated by the
438 kidneys and highly internalized by the reticuloendothelial system. Furthermore, even if
439 the target cells are reached, the negative charge and hydrophilic nature of siRNAs
440 strongly impair the cellular internalization (Castanotto and Rossi, 2009; Moreira et al.,
441 2008). Such limitations emphasize the need for an efficient and safe system to modulate
442 the siRNA pharmacokinetics and biodistribution.

443 In this respect, SALP (Maurer et al., 2001; Semple et al., 2001) and SNALP (Akinc et
444 al., 2010; Geisbert et al., 2006; Judge et al., 2009; Morrissey et al., 2005; Zimmermann
445 et al., 2006) fulfilled some of the requisites that should be present in a nanoparticle for
446 intravenous administration of siRNA such as, high encapsulation efficiency, protection
447 against nucleases, a small mean size, charge close to the neutrality and, prolonged blood
448 circulation times. Nevertheless, those features are not enough to dictate an effective
449 systemic siRNA delivery to distant sites of disease, like solid tumors localized in organs
450 other than the liver. Actually, most of the studies involving sterically stabilized
451 liposomes containing nucleic acids demonstrated that these particles naturally
452 accumulate in the liver and spleen (Akinc et al., 2010; Geisbert et al., 2006; Judge et al.,
453 2009; Kim et al., 2007; Morrissey et al., 2005; Zimmermann et al., 2006), being the
454 accumulation into solid tumors still an enormous challenge. Despite this constraint, the
455 aforementioned classes of liposomes represent an opportunity for further improvements
456 on the targeted delivery to solid tumors upon covalently coupling of ligands targeting
457 internalizing receptors. Antagonist G (Santos et al., 2010), transferrin (Mendonca et
458 al., 2010) and folate (Yang et al., 2004) are examples of ligands which have been
459 explored as targeting devices of nanoparticles of different nature, including liposomes
460 similar to the ones herein described. However, these strategies aiming at targeting
461 cancer cells have not increased the level of tumor accumulation, in comparison to their
462 non-targeted counterpart, but rather the intracellular delivery of those liposomes that

463 were able to cross the leaky tumor endothelium. In the work of Moreira et al. (Moreira
464 et al., 2001a; Moreira et al., 2001b), tumor accumulation of antagonist G-targeted
465 liposomes and the non-targeted counterpart was similar, despite the enhanced cellular
466 internalization observed *in vitro* of the former. Moreover, Bartlett et al. (Bartlett et al.,
467 2007) also demonstrated that both non-targeted and transferrin-targeted siRNA
468 polymer-based nanoparticles exhibited similar biodistribution and tumor accumulation.
469 These results demonstrated that tumor accumulation of both cancer cell-targeted and
470 non-targeted nanoparticles was highly dependent on the EPR effect rather than on the
471 presence of a moiety targeting solely the cancer cells (Fang et al., 2011; Iyer et al.,
472 2006; Li and Huang, 2008).

473 Since endothelial cells from tumor blood vessels are more accessible to any nanoparticle
474 injected in the vascular compartment than cancer cells, and being aware of the
475 importance of angiogenesis for the tumor growth and metastasis formation, several
476 therapies targeting angiogenesis have been proposed as a complementary strategy to
477 treat cancer (Abdollahi and Folkman, 2010; Hadj-Slimane et al., 2007). Therefore, a
478 nanoparticle capable of guiding and concentrating a therapeutic siRNA into endothelial
479 cells from angiogenic tumor blood vessels, in addition to cancer cells, is expected to
480 result in improved tumor accumulation which ultimately will bring additional benefits
481 in the treatment of cancer.

482 The identification of receptors overexpressed on the surface of cancer cells as well as on
483 other cells that constitute the tumor microenvironment, gives rise to an avenue of
484 different forms for therapeutic intervention in oncology. The nucleolin receptor is one
485 of such target as it is overexpressed both on cancer cells and endothelial cells from the
486 angiogenic blood vessels (Christian et al., 2003). Therefore, the F3 peptide, which has
487 been demonstrated to be actively internalized by nucleolin, was chosen as the targeting
488 moiety (Porkka et al., 2002).

489 Overall, the developed F3-targeted sterically stabilized liposomes were characterized by
490 high nucleic acid encapsulation efficiency, ability to protect the encapsulated siRNA, a
491 mean size around 200 nm, homogeneous particle size distribution and a surface charge
492 close to neutrality, which are features that make these nanoparticles adequate for a
493 siRNA systemic administration.

494 Moreover, cellular association studies demonstrated that the attachment of the F3
495 peptide to the liposomal surface resulted in a specific and high extent of internalization
496 (more than 10-fold increase relative to the non-targeted counterpart) by both cancer and

497 endothelial cells from angiogenic blood vessels, but not by non-cancer BJ cells (Figures
498 2 and 3). However, it is important to point out that the improved uptake was not
499 necessarily synonymous of an efficient gene silencing, as reported by Santos et al.
500 (Santos et al., 2010). In this work, the improved cellular association of antagonist G-
501 targeted liposomes (similar to the ones used herein) and containing anti-*BCL2* siRNA,
502 has not enabled any gene silencing in small cell lung cancer cell lines.

503 In contrast, our eGFP silencing studies demonstrated a significant reduction of eGFP
504 expression in cells treated with anti-*eGFP* siRNA delivered by F3-targeted liposomes
505 (composed of 2 mol% of PEG), both at the protein and mRNA levels, whereas no
506 silencing was observed when cells were treated with the non-targeted counterpart. These
507 results thus indicated that the presence of the F3-peptide brings an important advantage
508 (Figures 3 and 6).

509 With the purpose of obtaining liposomes more stable in respect to size, higher amounts
510 of PEG (4 and 8 mol%) were tested. Despite the improvements achieved at the size
511 level (average reduction of 50 nm), the resulting F3-targeted liposomes were unable to
512 induce eGFP downregulation. Although PEG confers stability during the preparation
513 process and favourable pharmacokinetics characteristics *in vivo* (Semple et al., 2001),
514 Song et al. (Song et al., 2002) demonstrated that the incorporation of 5 mol% of Cer-
515 PEG in cationic liposomes complexed with plasmid or antisense oligonucleotides
516 (asODN), slightly impaired cellular internalization but severely inhibited the escape
517 from endosomes of the internalized nucleic acid, thus compromising the transfection
518 efficiency. After endocytosis, lipid mixing between liposomes and the endocytic
519 membrane has to occur, leading to the disruption of the endosomal membrane and the
520 subsequent release of the entrapped nucleic acid. However, the steric barrier imposed by
521 PEG strongly inhibits this process. This effect is more prominent when PEG is attached
522 to lipids with acyl chains longer than 14 C, as the dissociation rate from the liposomal
523 membrane is much slower. Similar results were also reported by others (Remaut et al.,
524 2007; Zhang et al., 1999) as well as for nanocarriers based on polyethylenimine and
525 cyclodextrin (Mishra et al., 2004). Despite this, as the present work aimed at
526 developing liposomes that could mediate systemic delivery of siRNA to breast tumors,
527 CerC₁₆-PEG₂₀₀₀ was deliberately used, since acyl chains longer than 14 C were also
528 associated with longer blood circulation times (Zhang et al., 1999).

529 Our results demonstrated a slight decrease on the rate of internalization of F3-targeted
530 liposomes formed with 8 mol% of PEG (Figure 4). However, the limiting step in respect
531 to gene silencing was rather the inability to escape from the endosomes, as revealed by
532 the observed co-localization between lysosomes and siRNA. These results have also
533 indicated that the lack of activity of the anti-*BCL2* siRNA delivered by antagonist G-
534 targeted liposomes previously mentioned (Santos et al., 2010) was probably due to the
535 presence of 10 mol% of CerC₁₆-PEG₂₀₀₀.

536 Taken together, these results demonstrated that with formulations that are internalized
537 through receptor-mediated endocytosis, as it happens with F3-targeted liposomes
538 containing siRNA (Moura et al., 2011), a careful selection of the PEG-derivatized lipid
539 content is required. This demand aims at guaranteeing liposomal size stability without
540 compromising their ability to release the siRNA into the cell cytoplasm, where the RNA
541 interference machinery is located.

542 Alternatively, it is interesting to notice that the obstacles imposed by the presence of
543 high amounts of PEG, in this type of formulation, can be overcome through the
544 selection of targeting ligands (such as transferrin) with fusogenic properties (da Cruz et
545 al., 2001). In fact, Mendonça et al. (Mendonca et al., 2010) have developed transferrin-
546 targeted liposomes, similar to the liposomes described herein but formed with 8 mol%
547 of PEG, which *in vitro* resulted in *BCR-ABL* silencing, at the mRNA and protein levels,
548 in two leukemia cell lines. Moreover, Yang et al. (Yang et al., 2004) have also achieved
549 downregulation of EGFR upon treatment of KB cells with folate-targeted liposomes,
550 composed with 10 mol% of PEG, indicating that folate, like transferrin, can also have
551 some fusogenic properties at acidic pH. Nevertheless, and as discussed, such strategies
552 targeting only cancer cells are not likely to significantly improved *in vivo* tumor
553 accumulation.

554 Overall, the developed F3-targeted liposomes presented adequate features for
555 intravenous administration of siRNA and led to a significant improvement in the
556 internalization by both cancer and endothelial cells from angiogenic blood vessels,
557 which was further correlated with an effective gene silencing. The present work
558 represents an important contribution towards a nanoparticle with multi-targeting
559 capabilities, both at the cellular and molecular level.

560

561 **Acknowledgements**

562 The authors would like to acknowledge Nuno Fonseca for his helpful discussion of this
563 manuscript.

564 LÍgia C. Gomes-da-Silva and Adriana O. Santos were students of the international PhD
565 program on Biomedicine and Experimental Biology from the Center for Neurosciences
566 and Cell Biology and recipients of fellowship from the Portuguese Foundation for
567 Science and Technology (FCT) (ref.: SFRH/BD/33184/2007 and
568 SFRH/BD/11817/2003, respectively). The work was supported by the Portugal-Spain
569 capacitation program in Nanoscience and Nanotechnology (ref.: NANO/NMed-
570 AT/0042/2007).

571

572 **References**

573 Abdollahi, A., and Folkman, J. 2010. Evading tumor evasion: current concepts and
574 perspectives of anti-angiogenic cancer therapy. *Drug Resist Updat* 13, 16-28.

575 Akinc, A., Querbes, W., De, S., Qin, J., Frank-Kamenetsky, M., Jayaprakash, K.N., Jayaraman,
576 M., Rajeev, K.G., Cantley, W.L., Dorkin, J.R., et al. 2010. Targeted delivery of RNAi therapeutics
577 with endogenous and exogenous ligand-based mechanisms. *Mol Ther* 18, 1357-1364.

578 Allen, T.M., and Hansen, C. 1991. Pharmacokinetics of stealth versus conventional
579 liposomes: effect of dose. *Biochim Biophys Acta* 1068, 133-141.

580 Allen, T.M., Hansen, C., Martin, F., Redemann, C., and Yau-Young, A. 1991. Liposomes
581 containing synthetic lipid derivatives of poly(ethylene glycol) show prolonged circulation half-
582 lives in vivo. *Biochim Biophys Acta* 1066, 29-36.

583 Bartlett, D.W., Su, H., Hildebrandt, I.J., Weber, W.A., and Davis, M.E. 2007. Impact of
584 tumor-specific targeting on the biodistribution and efficacy of siRNA nanoparticles measured
585 by multimodality in vivo imaging. *Proc Natl Acad Sci U S A* 104, 15549-15554.

586 Bumcrot, D., Manoharan, M., Koteliansky, V., and Sah, D.W. 2006. RNAi therapeutics: a
587 potential new class of pharmaceutical drugs. *Nat Chem Biol* 2, 711-719.

588 Castanotto, D., and Rossi, J.J. 2009. The promises and pitfalls of RNA-interference-based
589 therapeutics. *Nature* 457, 426-433.

590 Christian, S., Pilch, J., Akerman, M.E., Porkka, K., Laakkonen, P., and Ruoslahti, E. 2003.
591 Nucleolin expressed at the cell surface is a marker of endothelial cells in angiogenic blood
592 vessels. *J Cell Biol* 163, 871-878.

593 da Cruz, M.T., Simoes, S., Pires, P.P., Nir, S., and de Lima, M.C. 2001. Kinetic analysis of the
594 initial steps involved in lipoplex-cell interactions: effect of various factors that influence
595 transfection activity. *Biochim Biophys Acta* 1510, 136-151.

596 Di Paolo, D., Ambrogio, C., Pastorino, F., Brignole, C., Martinengo, C., Carosio, R., Loi, M.,
597 Pagnan, G., Emionite, L., Cilli, M., et al. 2011. Selective Therapeutic Targeting of the Anaplastic
598 Lymphoma Kinase With Liposomal siRNA Induces Apoptosis and Inhibits Angiogenesis in
599 Neuroblastoma. *Mol Ther* 19, 2201-2212.

600 Elbashir, S.M., Harborth, J., Lendeckel, W., Yalcin, A., Weber, K., and Tuschl, T. 2001a.
601 Duplexes of 21-nucleotide RNAs mediate RNA interference in cultured mammalian cells.
602 *Nature* 411, 494-498.

603 Elbashir, S.M., Lendeckel, W., and Tuschl, T. 2001b. RNA interference is mediated by 21-
604 and 22-nucleotide RNAs. *Genes Dev* 15, 188-200.

605 Fang, J., Nakamura, H., and Maeda, H. 2011. The EPR effect: Unique features of tumor
606 blood vessels for drug delivery, factors involved, and limitations and augmentation of the
607 effect. *Adv Drug Deliv Rev* 63, 136-151.

- 608 Fire, A., Xu, S., Montgomery, M.K., Kostas, S.A., Driver, S.E., and Mello, C.C. 1998. Potent
609 and specific genetic interference by double-stranded RNA in *Caenorhabditis elegans*. *Nature*
610 391, 806-811.
- 611 Geisbert, T.W., Hensley, L.E., Kagan, E., Yu, E.Z., Geisbert, J.B., Daddario-DiCaprio, K., Fritz,
612 E.A., Jahrling, P.B., McClintock, K., Phelps, J.R., et al. 2006. Postexposure protection of guinea
613 pigs against a lethal ebola virus challenge is conferred by RNA interference. *J Infect Dis* 193,
614 1650-1657.
- 615 Hadj-Slimane, R., Lepelletier, Y., Lopez, N., Garbay, C., and Raynaud, F. 2007. Short
616 interfering RNA (siRNA), a novel therapeutic tool acting on angiogenesis. *Biochimie* 89, 1234-
617 1244.
- 618 Hanahan, D., and Weinberg, R.A. 2011. Hallmarks of cancer: the next generation. *Cell* 144,
619 646-674.
- 620 Hutvagner, G., and Zamore, P.D. 2002. A microRNA in a multiple-turnover RNAi enzyme
621 complex. *Science* 297, 2056-2060.
- 622 Ishida, T., Iden, D.L., and Allen, T.M. 1999. A combinatorial approach to producing sterically
623 stabilized (Stealth) immunoliposomal drugs. *FEBS Lett* 460, 129-133.
- 624 Iyer, A.K., Khaled, G., Fang, J., and Maeda, H. 2006. Exploiting the enhanced permeability
625 and retention effect for tumor targeting. *Drug Discov Today* 11, 812-818.
- 626 Jemal, A., Bray, F., Center, M.M., Ferlay, J., Ward, E., and Forman, D. 2011. Global cancer
627 statistics. *CA Cancer J Clin* 61, 69-90.
- 628 Judge, A.D., Robbins, M., Tavakoli, I., Levi, J., Hu, L., Fronda, A., Ambegia, E., McClintock, K.,
629 and MacLachlan, I. 2009. Confirming the RNAi-mediated mechanism of action of siRNA-based
630 cancer therapeutics in mice. *J Clin Invest* 119, 661-673.
- 631 Kim, S.I., Shin, D., Choi, T.H., Lee, J.C., Cheon, G.J., Kim, K.Y., Park, M., and Kim, M. 2007.
632 Systemic and specific delivery of small interfering RNAs to the liver mediated by apolipoprotein
633 A-I. *Mol Ther* 15, 1145-1152.
- 634 Li, S.D., and Huang, L. 2008. Pharmacokinetics and biodistribution of nanoparticles. *Mol*
635 *Pharm* 5, 496-504.
- 636 Li, X., Zhao, X., Fang, Y., Jiang, X., Duong, T., Fan, C., Huang, C.C., and Kain, S.R. 1998.
637 Generation of destabilized green fluorescent protein as a transcription reporter. *J Biol Chem*
638 273, 34970-34975.
- 639 Marchio, S., Lahdenranta, J., Schlingemann, R.O., Valdembri, D., Wesseling, P., Arap, M.A.,
640 Hajitou, A., Ozawa, M.G., Trepel, M., Giordano, R.J., et al. 2004. Aminopeptidase A is a
641 functional target in angiogenic blood vessels. *Cancer Cell* 5, 151-162.
- 642 Maurer, N., Wong, K.F., Stark, H., Louie, L., McIntosh, D., Wong, T., Scherrer, P., Semple,
643 S.C., and Cullis, P.R. 2001. Spontaneous entrapment of polynucleotides upon electrostatic
644 interaction with ethanol-destabilized cationic liposomes. *Biophys J* 80, 2310-2326.
- 645 Mendonca, L.S., Firmino, F., Moreira, J.N., Pedrosa de Lima, M.C., and Simoes, S. 2010.
646 Transferrin receptor-targeted liposomes encapsulating anti-BCR-ABL siRNA or asODN for
647 chronic myeloid leukemia treatment. *Bioconjug Chem* 21, 157-168.
- 648 Mishra, S., Webster, P., and Davis, M.E. 2004. PEGylation significantly affects cellular
649 uptake and intracellular trafficking of non-viral gene delivery particles. *Eur J Cell Biol* 83, 97-
650 111.
- 651 Moreira, J.N., Gaspar, R., and Allen, T.M. 2001a. Targeting Stealth liposomes in a murine
652 model of human small cell lung cancer. *Biochim Biophys Acta* 1515, 167-176.
- 653 Moreira, J.N., Hansen, C.B., Gaspar, R., and Allen, T.M. 2001b. A growth factor antagonist as
654 a targeting agent for sterically stabilized liposomes in human small cell lung cancer. *Biochim*
655 *Biophys Acta* 1514, 303-317.
- 656 Moreira, J.N., Ishida, T., Gaspar, R., and Allen, T.M. 2002. Use of the post-insertion
657 technique to insert peptide ligands into pre-formed stealth liposomes with retention of
658 binding activity and cytotoxicity. *Pharm Res* 19, 265-269.

- 659 Moreira, J.N., Santos, A., Moura, V., Pedroso de Lima, M.C., and Simoes, S. 2008. Non-viral
660 lipid-based nanoparticles for targeted cancer systemic gene silencing. *J Nanosci Nanotechnol* 8,
661 2187-2204.
- 662 Morrissey, D.V., Lockridge, J.A., Shaw, L., Blanchard, K., Jensen, K., Breen, W., Hartsough, K.,
663 Machermer, L., Radka, S., Jadhav, V., et al. 2005. Potent and persistent in vivo anti-HBV activity
664 of chemically modified siRNAs. *Nat Biotechnol* 23, 1002-1007.
- 665 Moura, V., Lacerda, M., Figueiredo, P., Corvo, M.L., Cruz, M.E., Soares, R., de Lima, M.C.,
666 Simoes, S., and Moreira, J.N. 2011. Targeted and intracellular triggered delivery of therapeutics
667 to cancer cells and the tumor microenvironment: impact on the treatment of breast cancer.
668 *Breast Cancer Res Treat*.
- 669 Papahadjopoulos, D., Allen, T.M., Gabizon, A., Mayhew, E., Matthay, K., Huang, S.K., Lee,
670 K.D., Woodle, M.C., Lasic, D.D., Redemann, C., et al. 1991. Sterically stabilized liposomes:
671 improvements in pharmacokinetics and antitumor therapeutic efficacy. *Proc Natl Acad Sci U S*
672 *A* 88, 11460-11464.
- 673 Porkka, K., Laakkonen, P., Hoffman, J.A., Bernasconi, M., and Ruoslahti, E. 2002. A fragment
674 of the HMGN2 protein homes to the nuclei of tumor cells and tumor endothelial cells in vivo.
675 *Proc Natl Acad Sci U S A* 99, 7444-7449.
- 676 Remaut, K., Lucas, B., Braeckmans, K., Demeester, J., and De Smedt, S.C. 2007. Pegylation of
677 liposomes favours the endosomal degradation of the delivered phosphodiester
678 oligonucleotides. *J Control Release* 117, 256-266.
- 679 Santos, A.O., da Silva, L.C., Bimbo, L.M., de Lima, M.C., Simoes, S., and Moreira, J.N. 2010.
680 Design of peptide-targeted liposomes containing nucleic acids. *Biochim Biophys Acta* 1798,
681 433-441.
- 682 Semple, S.C., Klimuk, S.K., Harasym, T.O., Dos Santos, N., Ansell, S.M., Wong, K.F., Maurer,
683 N., Stark, H., Cullis, P.R., Hope, M.J., et al. 2001. Efficient encapsulation of antisense
684 oligonucleotides in lipid vesicles using ionizable aminolipids: formation of novel small
685 multilamellar vesicle structures. *Biochim Biophys Acta* 1510, 152-166.
- 686 Song, L.Y., Ahkong, Q.F., Rong, Q., Wang, Z., Ansell, S., Hope, M.J., and Mui, B. 2002.
687 Characterization of the inhibitory effect of PEG-lipid conjugates on the intracellular delivery of
688 plasmid and antisense DNA mediated by cationic lipid liposomes. *Biochim Biophys Acta* 1558,
689 1-13.
- 690 Torchilin, V.P. 2010. Passive and active drug targeting: drug delivery to tumors as an
691 example. *Handb Exp Pharmacol*, 3-53.
- 692 Yang, L., Li, J., Zhou, W., Yuan, X., and Li, S. 2004. Targeted delivery of antisense
693 oligodeoxynucleotides to folate receptor-overexpressing tumor cells. *J Control Release* 95,
694 321-331.
- 695 Zhang, Y.P., Sekirov, L., Saravolac, E.G., Wheeler, J.J., Tardi, P., Clow, K., Leng, E., Sun, R.,
696 Cullis, P.R., and Scherrer, P. 1999. Stabilized plasmid-lipid particles for regional gene therapy:
697 formulation and transfection properties. *Gene Ther* 6, 1438-1447.
- 698 Zimmermann, T.S., Lee, A.C., Akinc, A., Bramlage, B., Bumcrot, D., Fedoruk, M.N., Harborth,
699 J., Heyes, J.A., Jeffs, L.B., John, M., et al. 2006. RNAi-mediated gene silencing in non-human
700 primates. *Nature* 441, 111-114.

701
702

703 **Legends**

704 **Table 1.** Physico-chemical characterization of F3-targeted and non-targeted liposomes
705 containing anti-eGFP siRNA. Values are the mean \pm SD of at least 3 independent
706 experiments.

707

708 **Figure 1.** Extent of cellular association of rhodamine-labelled liposomes with human
709 cancer cell lines, endothelial cells and human fibroblasts analyzed by flow cytometry.
710 MDA-MB-435S and MDA-MB-231 cancer cells, human microvascular endothelial
711 cells (HMEC-1) or human non-cancer BJ fibroblasts (0.5×10^6) were incubated with
712 different concentrations of F3-targeted, targeted by a non-specific (NS) peptide and
713 non-targeted liposomes at A) 37°C or B) 37°C or 4°C, during 1 h. After incubation,
714 rhodamine signal was assessed by flow cytometry. Bars are the mean \pm SD of 3
715 independent experiments. Two-way ANOVA analysis of variance with Bonferroni's
716 post-test was used for comparison between the referenced samples and F3-targeted
717 liposomes. *** $p < 0.001$; ** $p < 0.01$; ns $p > 0.05$.

718

719 **Figure 2.** Cellular association of F3-targeted and non-targeted liposomes with human
720 cancer cell lines, endothelial cells and human fibroblasts, analyzed by confocal
721 microscopy. MDA-MB-435S and MDA-MB-231 cancer cells, human microvascular
722 endothelial cells (HMEC-1) or human non-cancer BJ fibroblasts (2.5×10^5) were
723 incubated with rhodamine-labelled (red) F3-targeted and non-targeted liposomes,
724 encapsulating FITC-labelled siRNA (green), at 0.2 mM of total lipid, during 1 h at 4 or
725 37°C. The nucleus was stained with DAPI (blue). Cells were fixed with 4%
726 paraformaldehyde, mounted in mowiol and visualized in a point scanning confocal
727 microscope.

728

729 **Figure 3.** Effect of the number of transfections, poly(ethylene glycol) content or
730 treatment duration on eGFP levels. (A) MDA-MB-435S-eGFP and (B) MDA-MB-231-
731 eGFP cell lines were transfected twice with different concentrations of anti-eGFP
732 siRNA encapsulated in F3-targeted or non-targeted liposomes, incorporating 2 mol% of
733 CerC₁₆-PEG₂₀₀₀. A non-specific siRNA encapsulated in F3-targeted liposomes was
734 included as control (CTR). Alternatively, only a single treatment was performed. EGFP
735 levels were evaluated by flow cytometry 96 h after the beginning of the experiment. (C)
736 EGFP levels were evaluated 48 h after one single treatment with liposomes composed
737 of 2 mol% of CerC₁₆-PEG₂₀₀₀. (D) MDA-MB-435-eGFP cells were transfected twice as
738 in A) but with liposomes formed with 4 mol% of CerC₁₆-PEG₂₀₀₀. Bars are the mean \pm
739 SEM of 3 independent experiments. Two-way ANOVA analysis of variance with
740 Bonferroni's post-test was used for multiple comparisons. Asterisk symbols represented

741 the significance level of the difference between the referenced formulations and F3-
742 targeted liposomes containing the anti-*eGFP* siRNA (** $p < 0.001$; ** $p < 0.01$; * $p < 0.05$);
743 *cardinal* symbols represented the significance level of the difference between *eGFP*
744 levels at the referenced time point (#### $p < 0.001$) when comparison was established
745 between *eGFP* silencing at 48 h and 96 h.

746

747 **Figure 4.** Effect of PEG content on the extent of cellular association of F3-targeted
748 liposomes by MDA-MB-435S cancer and HMEC-1 endothelial cells. Half-million cells
749 were incubated with rhodamine-labelled F3-targeted liposomes incorporating 2 or 8
750 mol% of CerC₁₆-PEG₂₀₀₀, at 0.2 mM of total lipid, for 1 h at 37°C. After incubation,
751 rhodamine signal was assessed by flow cytometry. Bars are the mean \pm SD of 3
752 independent experiments. One-way ANOVA analysis of variance with Bonferroni's
753 post-test was used for comparison between F3-targeted liposomes incorporating 2 and 8
754 mol% of PEG (ns $p > 0.05$).

755

756 **Figure 5.** Intracellular trafficking of siRNA encapsulated in F3-targeted liposomes.
757 Cells were incubated with liposomes prepared either with A) 8 or B) 2 mol% of PEG,
758 containing a FITC-labelled siRNA (green), during 4 h at 37°C. Afterwards, lysosomes
759 were labeled with LysoTracker Red (red) and live cells visualized in a point scanning
760 confocal microscope.

761

762 **Figure 6.** Effect of anti-*eGFP* siRNA encapsulated in different liposomal formulations
763 on the *eGFP* mRNA in MDA-MB-435S-*eGFP* cells. Cells were transfected at 0 and 48
764 h, with either anti-*eGFP* siRNA encapsulated in F3-targeted or non-targeted liposomes,
765 containing 2 mol% of CerC₁₆-PEG₂₀₀₀, or with the control siRNA encapsulated in the
766 former. *EGFP* mRNA levels were assessed 24 h after the second transfection by qRT-
767 PCR and in comparison with the mRNA levels of untreated cells. Bars are the mean \pm
768 SD of 3 independent experiments. Two-way ANOVA analysis of variance with
769 Bonferroni's post-test was used for comparison between the referenced samples and F3-
770 targeted liposomes containing the anti-*eGFP* siRNA (** $p < 0.01$, * $p < 0.05$).

771

772

772 **Table 1**

PEG (mol%)	F3-targeted liposomes			Non-targeted liposomes		
	Size (nm)	Polidispersity index	Encaps. efficiency (%)	Size (nm)	Polidispersity index	Encaps. efficiency (%)
2	254.4 ± 26.55	0.144 ± 0.03	95.72 ± 8.44	130.3 ± 13.32	0.076 ± 0.05	99.77 ± 8.48
4	194.7 ± 16.40	0.149 ± 0.03	95.99 ± 21.15	109.0 ± 10.82	0.145 ± 0.05	90.32 ± 12.42
8	210.2 ± 21.74	0.146 ± 0.06	76.86 ± 16.63	112.1 ± 4.51	0.281 ± 0.05	87.53 ± 18.32

773

774

775

776

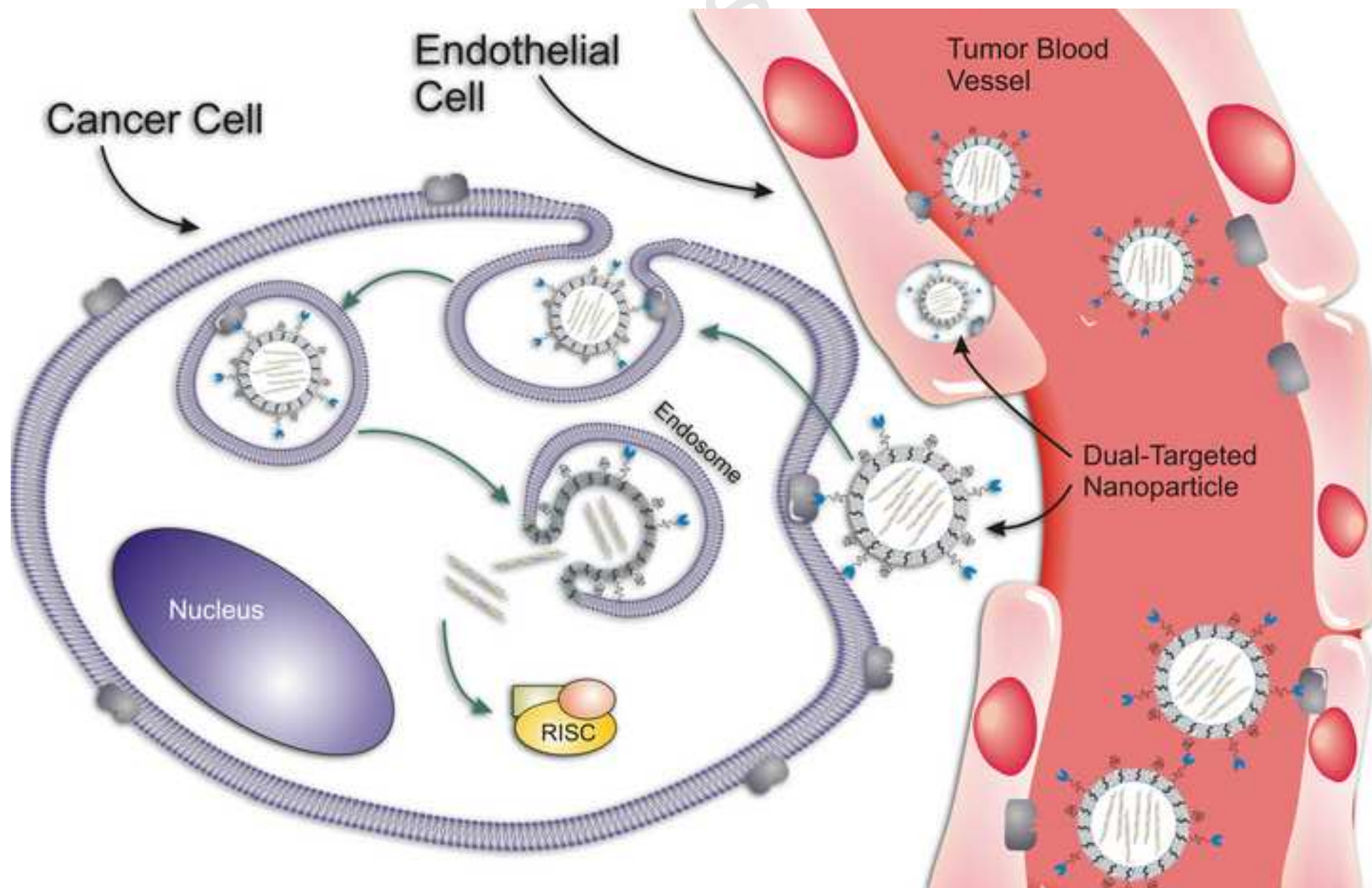
777

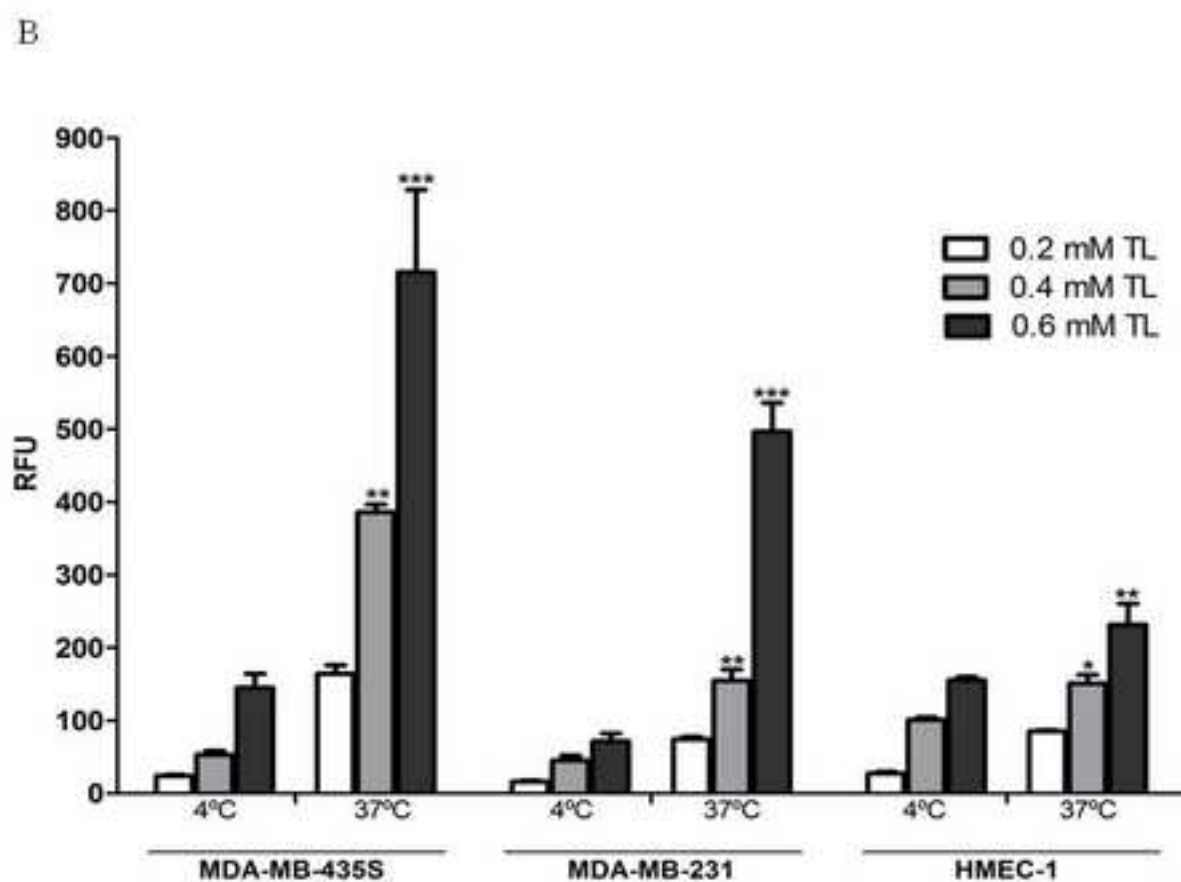
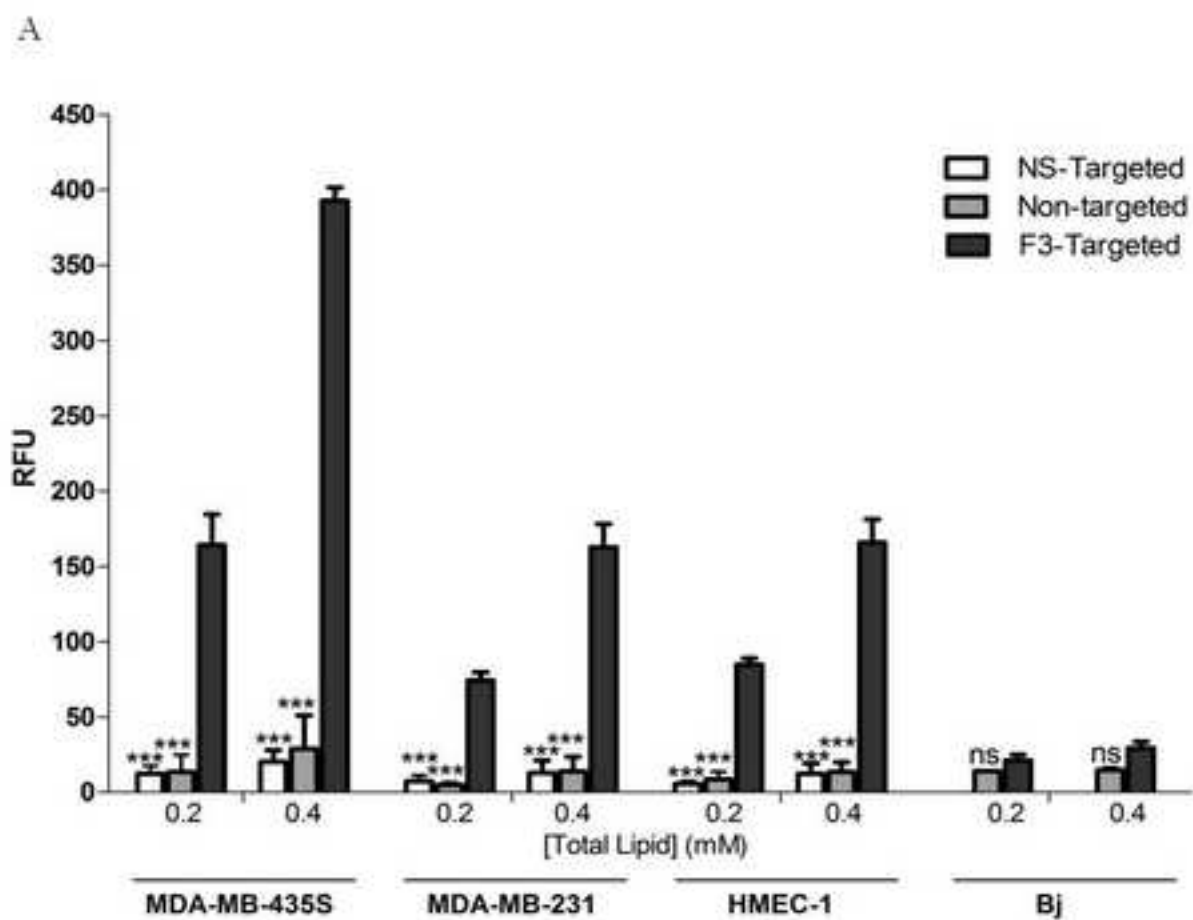
778

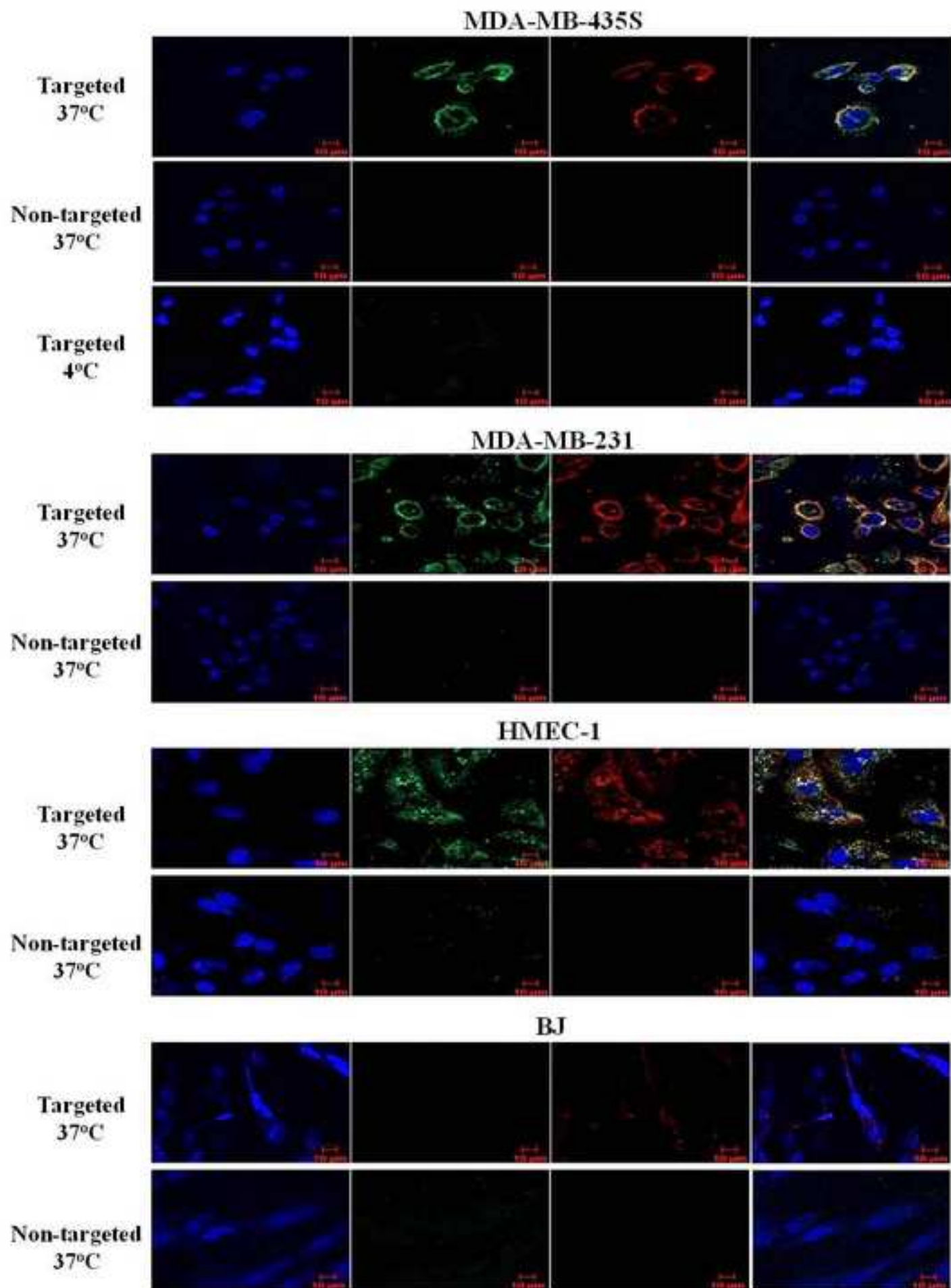
779

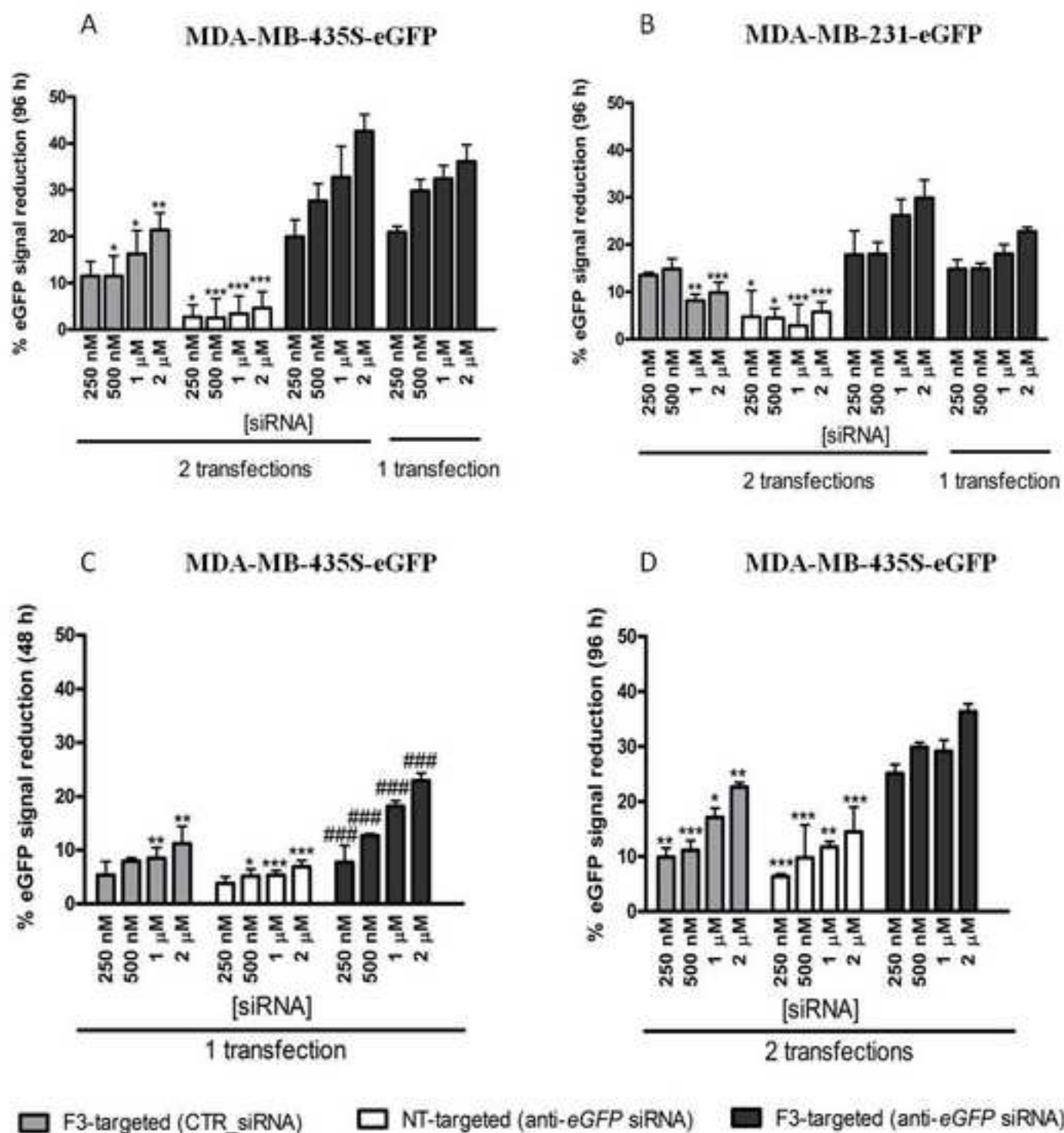
780

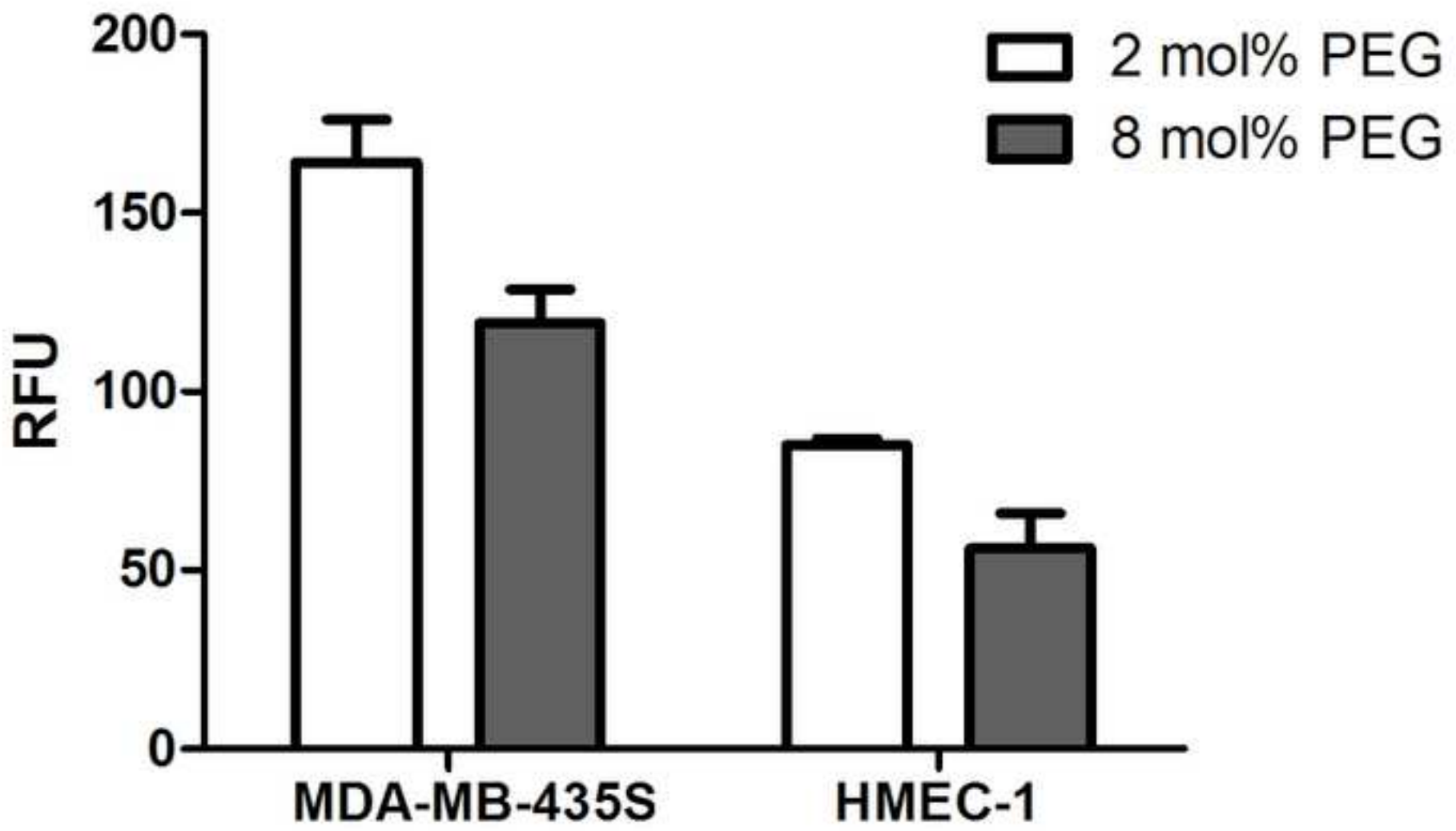
781











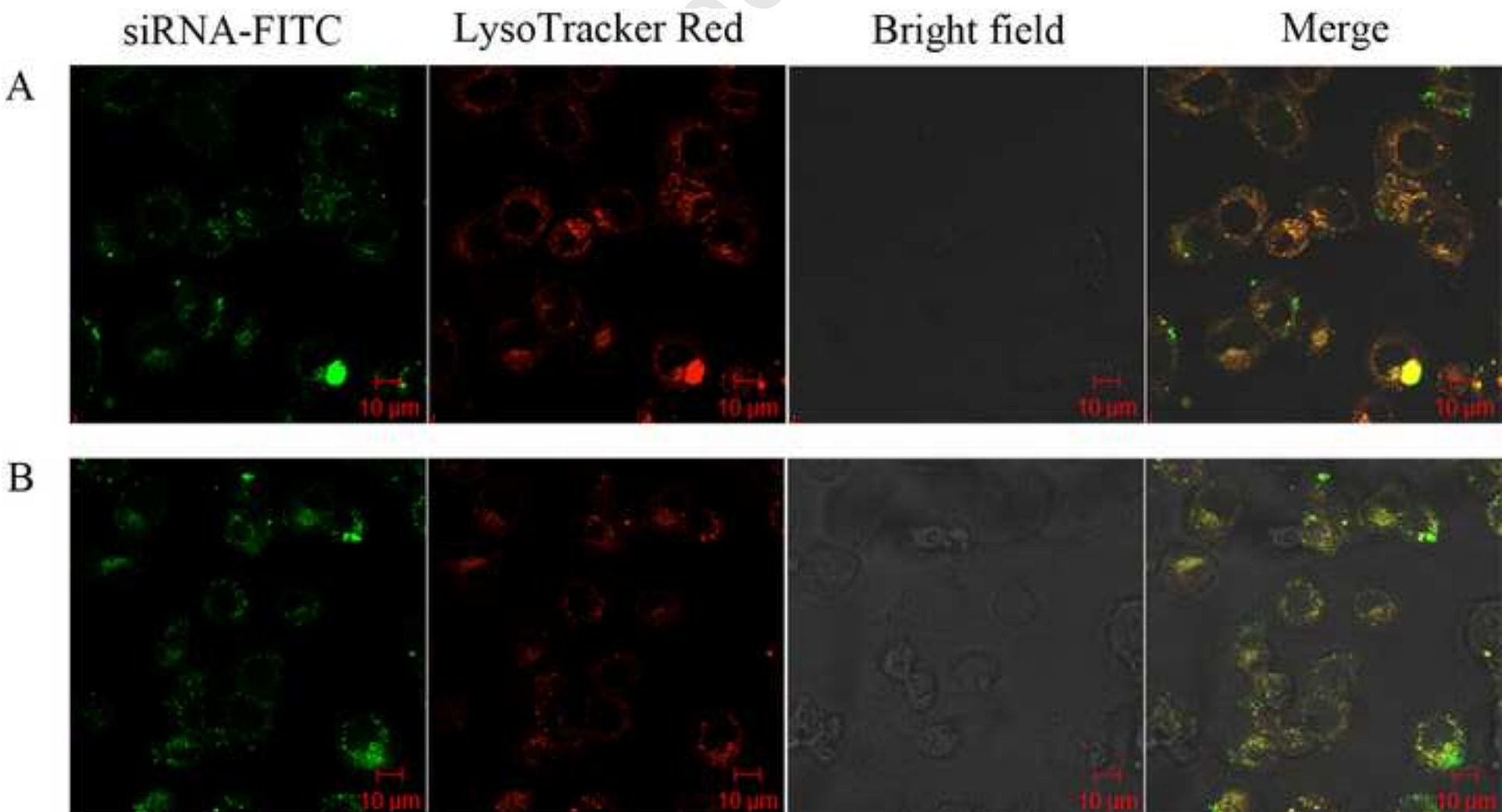
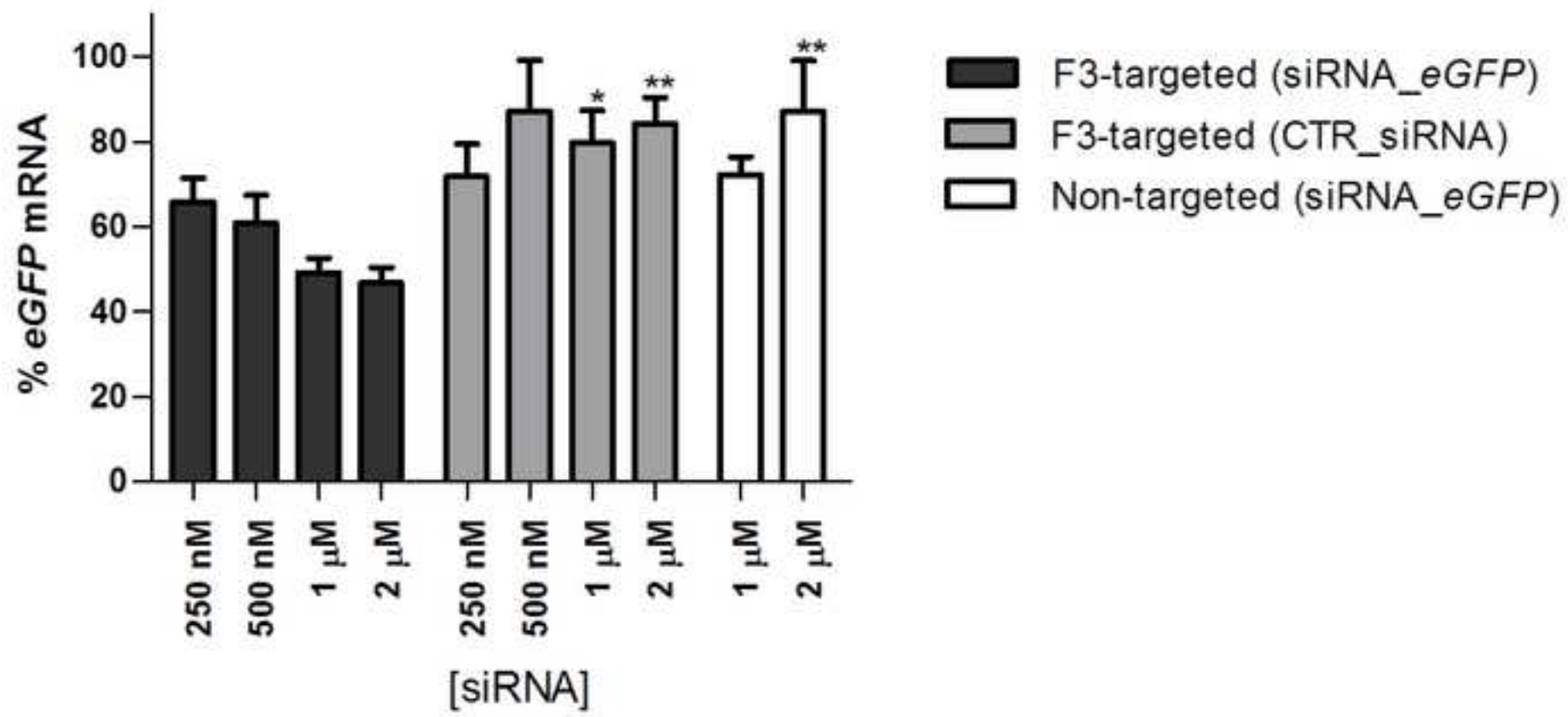
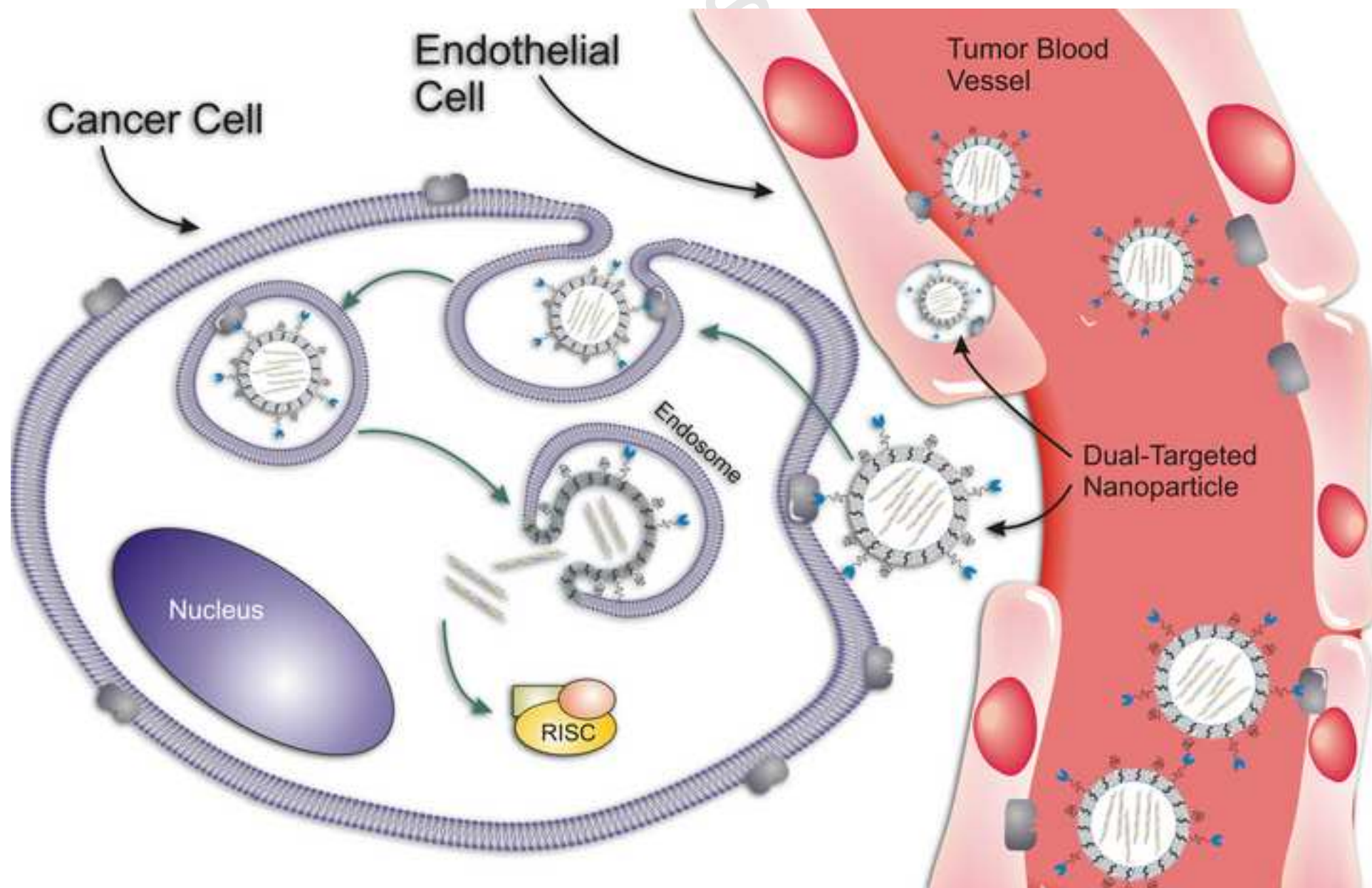
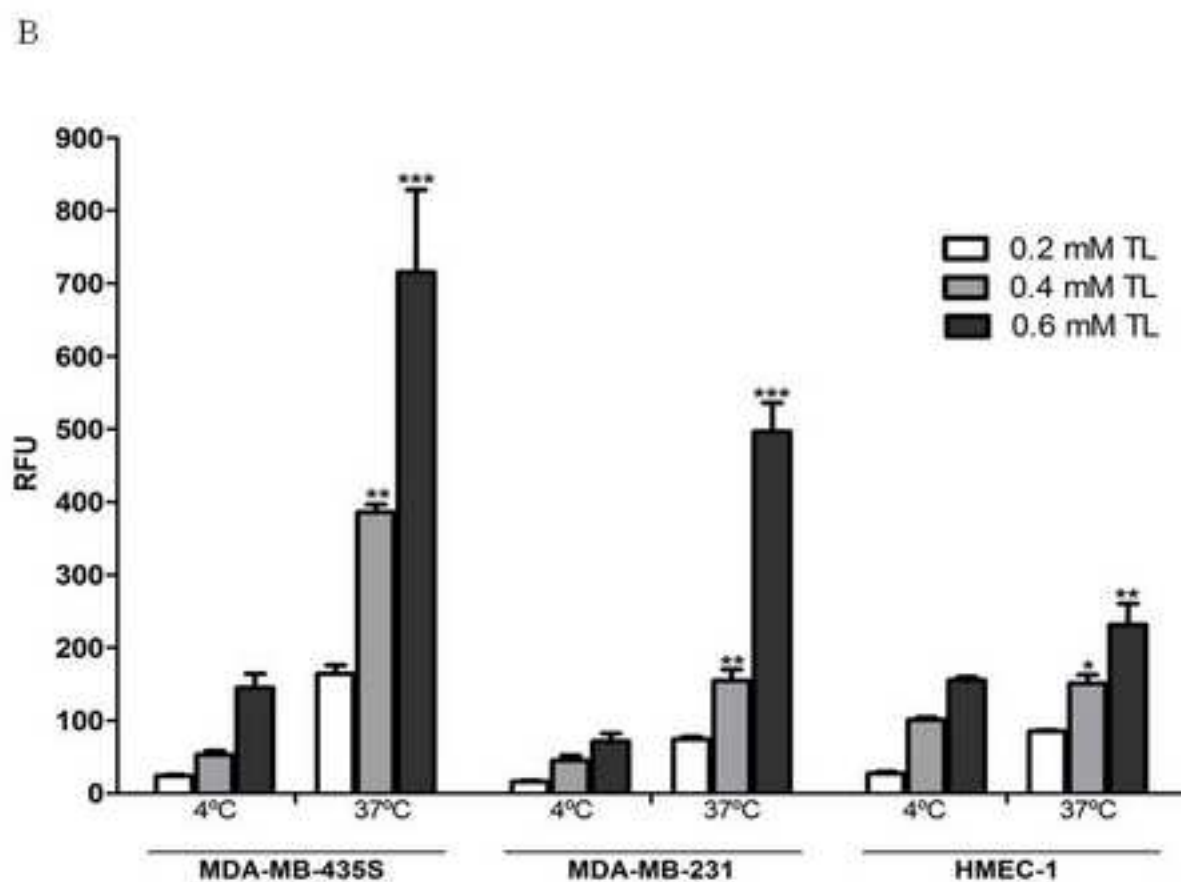
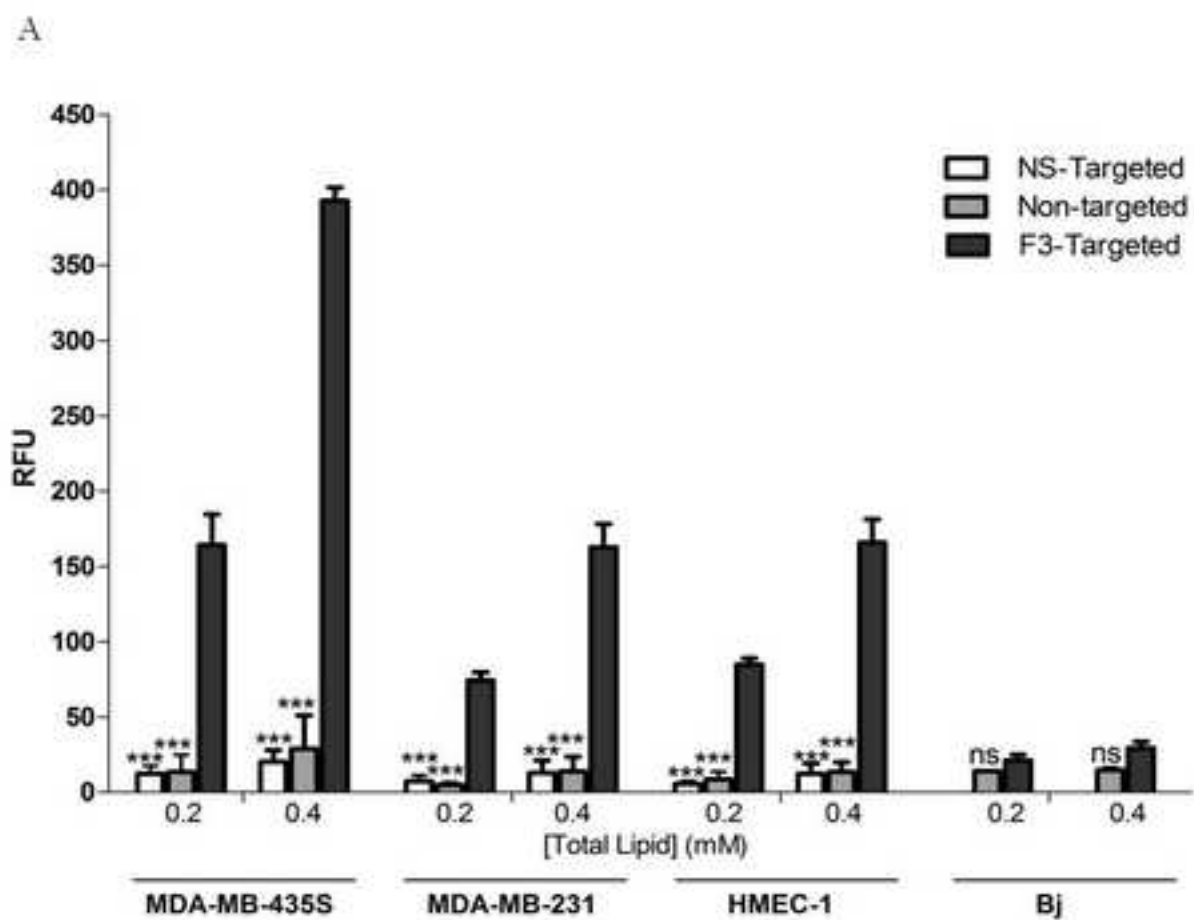
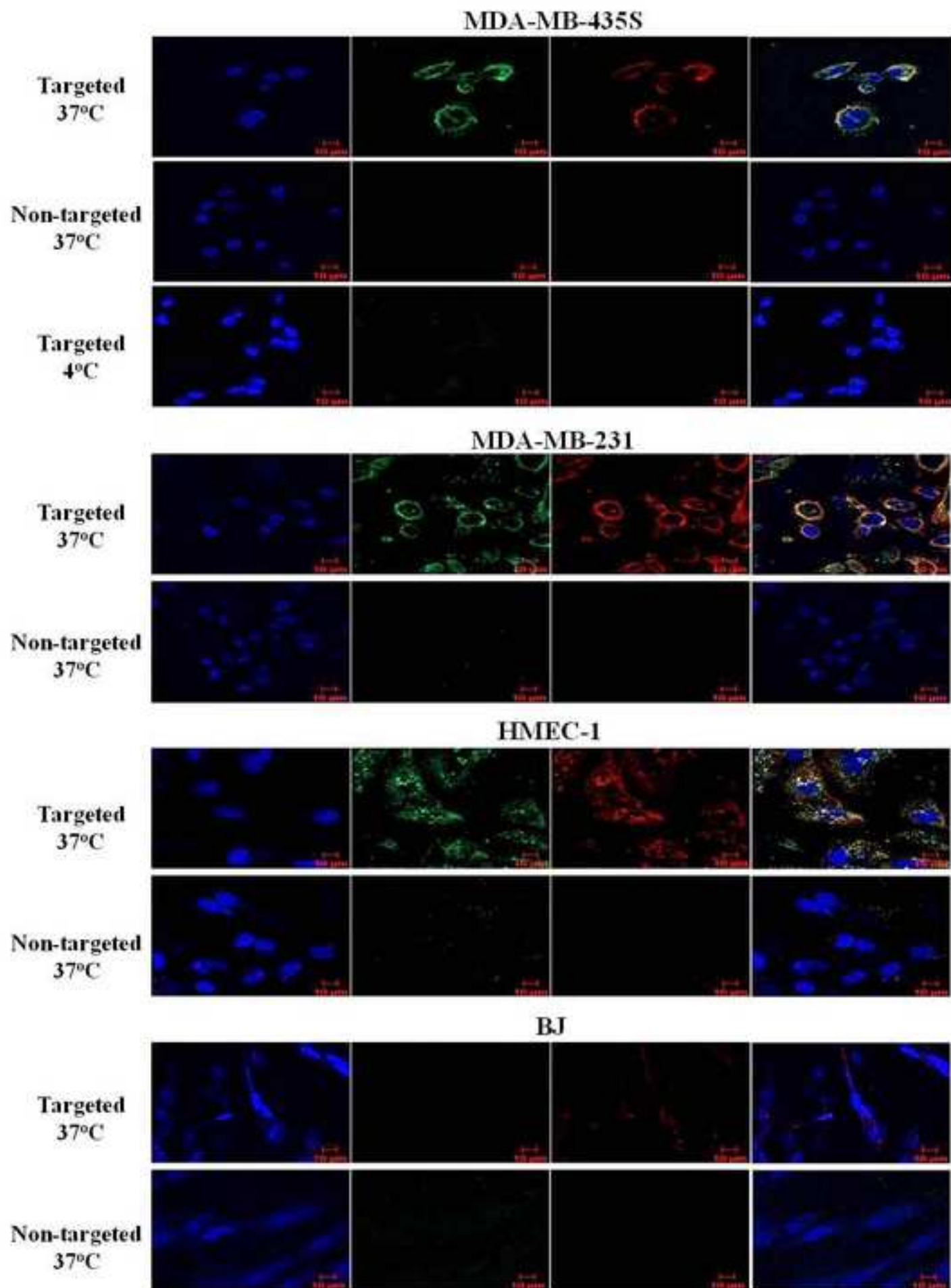


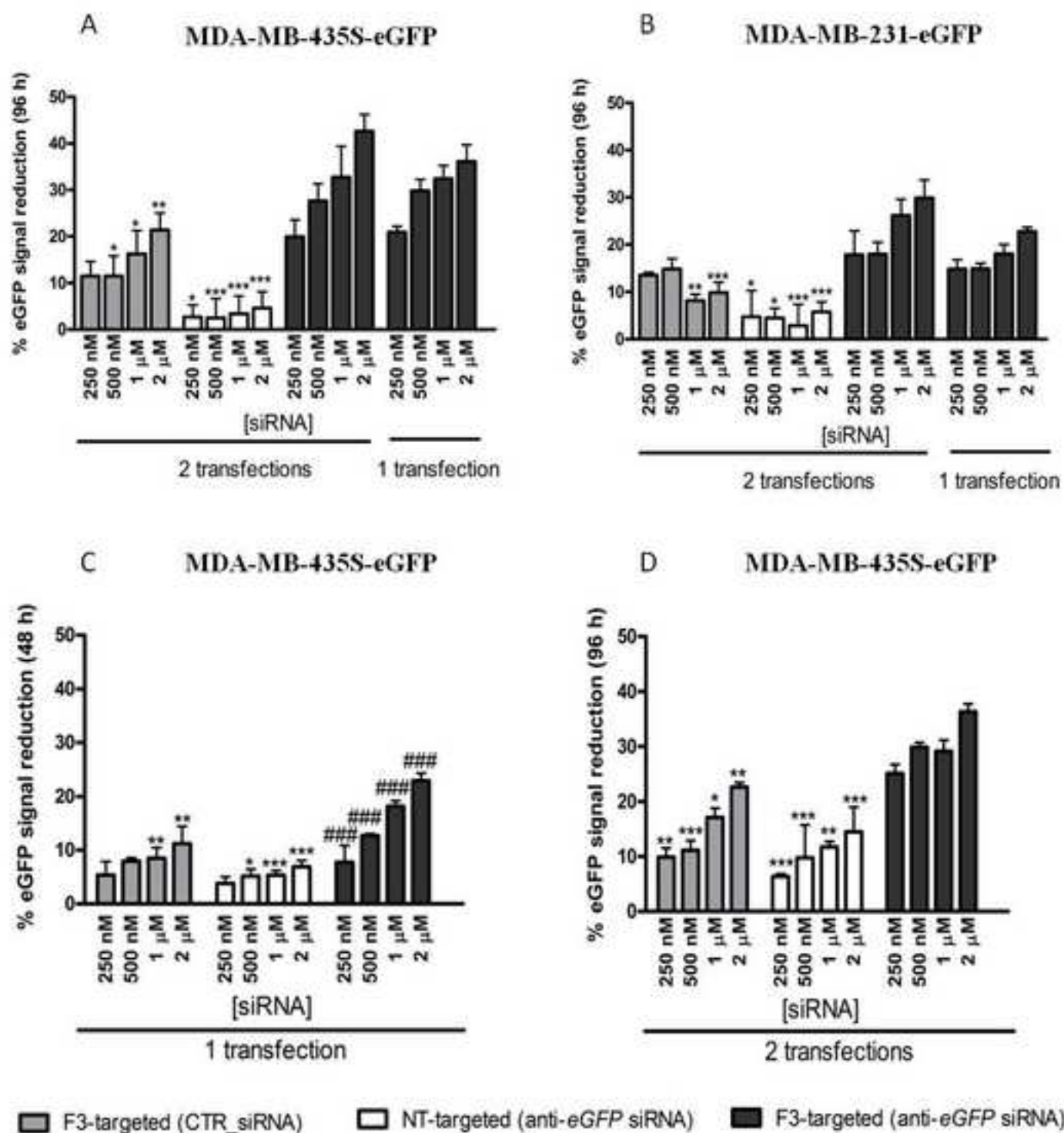
Figure 6











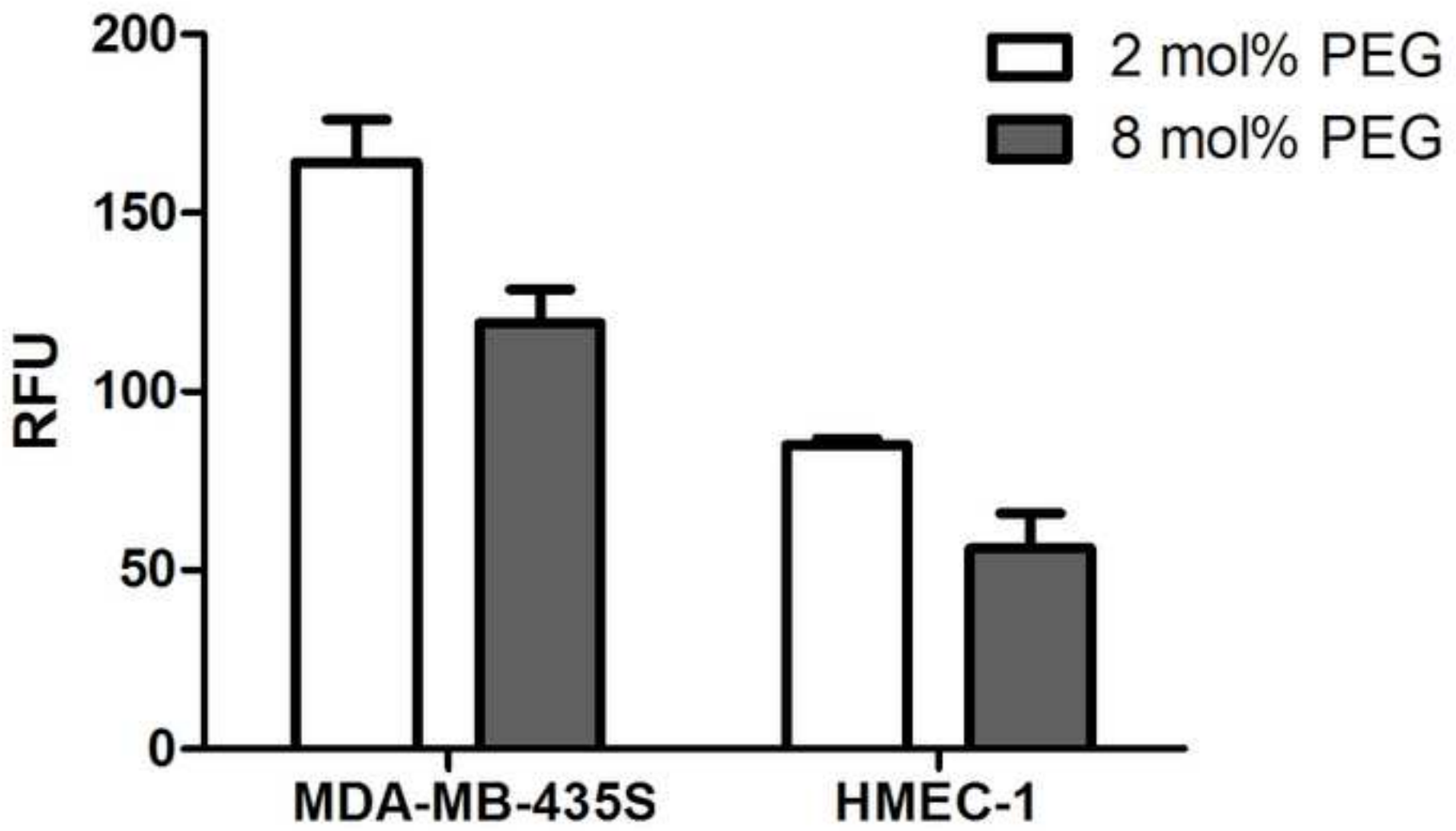


Figure 5

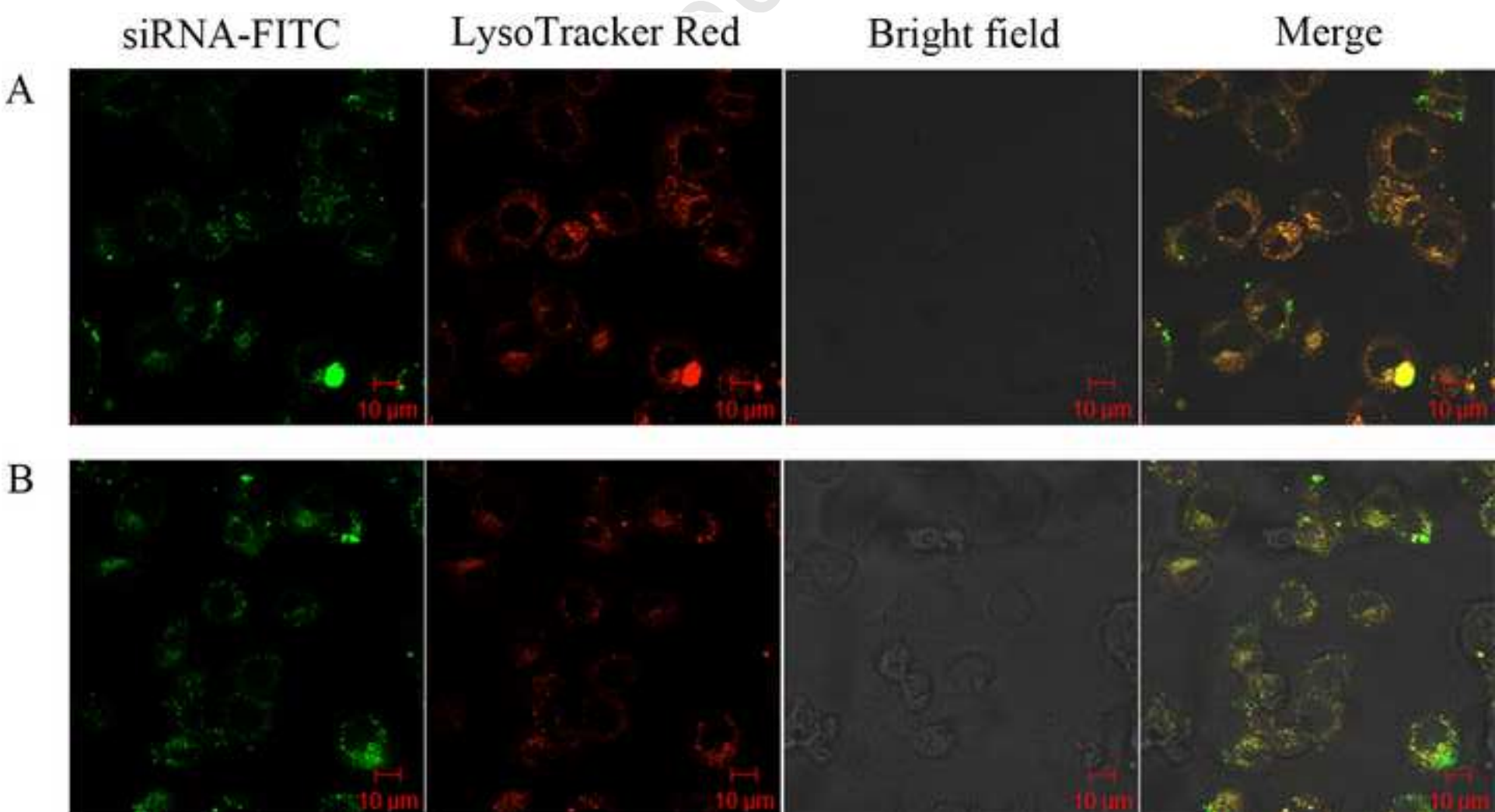


Figure 6

